Working at the limit: A review of thermodynamics and optimality of the Earth system

Axel Kleidon[1]

[1]Max-Planck-Institute for Biogeochemistry, Hans-Knoell-Str. 10, 07745 Jena, Germany

Correspondence: Axel Kleidon (akleidon@bgc-jena.mpg.de)

Abstract. Optimality concepts related to energy and entropy have long been proposed in Earth system science, yet they remain obscure, seem contradictory regarding their goal to either maximize or minimize, and have so far only played marginal roles. This review aims to clarify the role of thermodynamics and optimality in Earth system science by showing that it plays a pivotal role in how, and how much, work can be derived from the solar forcing, and that this imposes a major constraint to the

5   dynamics of dissipative structures of the Earth system. This is, however, not as simple as it may sound. It requires a consistent formulation of Earth system processes in thermodynamic terms, including their linkages and interactions. Thermodynamics then constrains the ability of the Earth system to derive work and generate free energy from the solar radiative forcing, which limits the ability to maintain motion, mass transport, geochemical cycling, and biotic activity. It thus limits directly the generation of atmospheric motion and other processes indirectly through their need for transport, such as hydrologic cycling or biotic

10   activity. I demonstrate the application of this thermodynamic Earth system view by deriving first-order estimates associated with atmospheric motion, hydrologic cycling, and terrestrial productivity that agree very well with observations. This supports the notion that the emergent simplicity and predictability inherent in observed climatological variations can be attributed to these processes working as hard as they can, reflecting thermodynamic limits directly or indirectly. I discuss how this thermodynamic interpretation is consistent with established theoretical concepts in the respective disciplines, interpret other optimality

15   concepts in light of this thermodynamic Earth system view, and describe its utility for Earth system science.

1   Introduction

The Earth system is an incredible complex system, with many processes interacting with each other, from the small, local scale up to the planetary scale. With human activity playing an increasing role, it appears that the system becomes even more complicated. This may seem to make the Earth a highly unpredictable and chaotic system, with arbitrary evolutionary directions

20   and outcomes. It would seem that the only contribution from physics to constrain the dynamics of this complex system comes from the basic conservation laws, as these provide the accounting basis for energy, mass, and momentum and other conserved quantities.

Yet, on the other hand, we observe various forms of relatively simple, emergent patterns in the Earth system that reflect highly predictable outcomes. Such emergent simplicity is, for instance, reflected in climate classifications (e.g. Koeppen, 1900),

25   typical surface energy balance partitioning and associated hydrologic classification schemes (Budyko, 1974), or the well-

documented variation of terrestrial biomes along gradients in climate (e.g. von Humboldt, 1845; Holdridge, 1947; Whittaker, 1962; Prentice et al., 1992). How does this simplicity emerge from the dynamics of such a complex system? It would seem that there are further constraints at play when it comes to such predictable aspects of the Earth system. Are these constraints arbitrary, too specific to the example being considered, or do they result from further physical constraints that are currently not

30   in the focus of our attention?

The aim of this paper is to demonstrate that it is thermodynamics which sets an additional, highly relevant constraint to the dynamics of the Earth system. This additional constraint is based on the explicit consideration of entropy and the second law of thermodynamics. Entropy is a key thermodynamic concept that describes, loosely speaking, how dispersed energy is at the microscopic scale of atoms and molecules (e.g., Atkins and de Paula, 2010). At this microscopic scale, energy is quantised,

35   distributed over discrete number of states. It is through the introduction of entropy and its maximisation that the microscopic distribution of energy is linked to macroscopic variables, such as temperature, density, and concentrations, that are commonly used to describe Earth system processes. Its central importance concerns two aspects: first, it provides a fundamental direction for energy conversions towards higher entropy, and second, it sets hard limits to the magnitude of the conversion, as reflected by the well-established Carnot limit. Every time energy is being converted on Earth, for instance, from solar radiation to heat

40   upon absorption, or from heat to kinetic energy when motion is generated, overall, entropy can only stay the same or increase, imposing a constraint known as the second law of thermodynamics.

How is this constraint going to play out? A series of publications consider the role of the second law in climate science (Ozawa et al., 2003; Singh and O'Neill, 2022) and ecology (Chapman et al., 2016; Nielsen et al., 2020), and related thermodynamic limits or optimality approaches, such as the proposed hypothesis of Maximum Entropy Production (MEP, e.g.,

45   Paltridge, 1975; Lorenz et al., 2001), maximum power (e.g., Lotka, 1922a, b; Odum and Pinkerton, 1955; Kleidon and Renner, 2013a), minimum entropy production (e.g., Prigogine, 1955; Essex, 1984), minimum dissipation (e.g., West et al., 1997, 1999) or energy expenditure (e.g., Rinaldo et al., 1992, 1996; Rodriguez-Iturbe and Rinaldo, 1997). The emergence of simple, predictable patterns in the climatological mean can then be attributed to processes evolving to and operating at such limits or optimal states. However, the applications have typically been to specific systems, and it is yet unresolved how general such

50   proposed optimality approaches are. For instance, the main application of MEP in climate science has been to atmospheric heat transport (Paltridge, 1975; Lorenz et al., 2001), while applications to other fields, such as hydrology have remained mostly at the conceptual (Kleidon and Schymanski, 2008) or semi-empirical level (Lin, 2010; Zehe et al., 2013). Also, other principles have been proposed that focus on the minimisation of energy expenditure in the context of river networks (e.g., Rinaldo et al., 1992, 1996; Rodriguez-Iturbe and Rinaldo, 1997) or frictional dissipation in vascular networks (West et al., 1997, 1999). In

55   the climatological mean, power balances dissipation, so the notion of maximising power or minimising dissipation seem rather contradictory to each other. It would thus seem that the thermodynamic organisation of Earth system processes do not fall under one, unifying thermodynamic organisation principle. It is then unclear which general insights could be gained from thermodynamics for the functioning of the Earth system.

This review summarises recent work to show that thermodynamics indeed strongly constrains the functioning of the Earth

60   system, resulting in the simplicity of the emergent climatological patterns and associated optimal functioning. This, however,
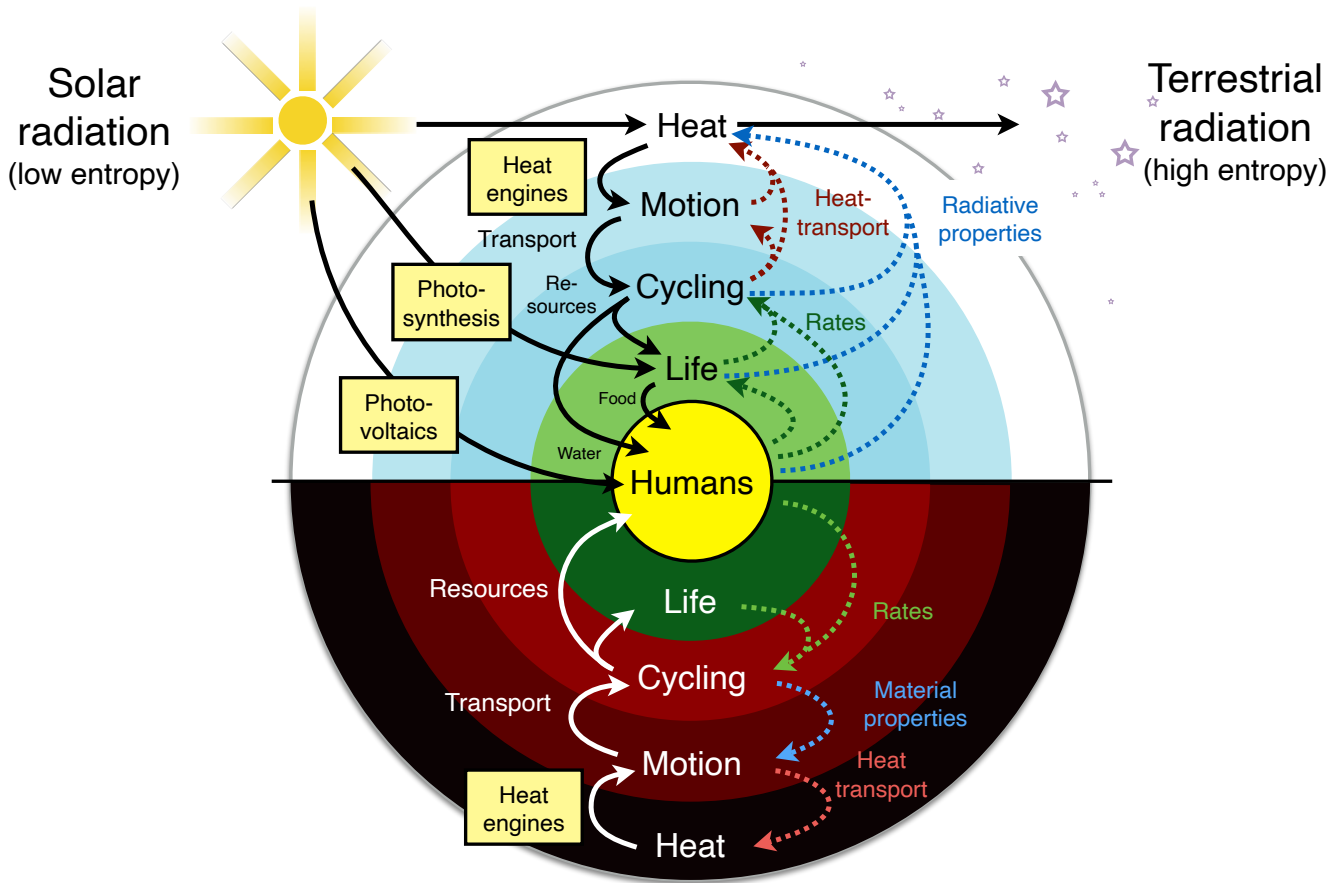
Figure 1. A hierarchical view of the Earth system in which thermodynamics constrains the process that generate free energy from low entropy sunlight (yellow boxes) that then fuels the dissipative dynamics of Earth system processes. Effects (dotted lines) of these processes feed back to the thermodynamic boundary conditions by transporting heat and changing radiative or material properties. Updated after Kleidon (2010; 2012; 2016).

requires a more differentiated view. This view contains three major components: (i) the concept of free energy, energy that results from work being done and that is free of entropy, (ii) the consequences of the dynamics, as these alter the boundary conditions under which free energy is generated, and (iii) optimality and resulting simplicity in climatological patterns being related primarily to the maximum power associated with the generation of motion and transport. This then results in a hierarchical view of the Earth system (Figure 1) that is driven by the low-entropy solar energy input, from which free energy can be generated by only a few mechanisms (as indicated by the yellow boxes in Figure 1). This drives sequences of further energy conversions and associated dynamics, which then feed back to the boundary conditions by transporting heat, changing rates, material properties, or radiative conditions. This picture of the Earth system is certainly more complex than simply stating that systems maximise or minimise some thermodynamic aspect. It nevertheless allows for a relatively simple way to be repre-

70 sented mathematically, it can be quantified, compared to observations and thus supported. We can then draw conclusions from it regarding the role of thermodynamic constraints and how these relate to optimality in the Earth system.

In the following, I first provide some basics of thermodynamics in Section 2 that are less common, but central for the thermodynamic description of the Earth system. These include the description of three forms of entropy which are obtained from the scaling of energy quanta in quantum physics (rather than just thermal entropy, which is central to classical thermodynamics),
75 a definition of free energy that is somewhat different to the concept of Gibbs (or Helmholtz) free energy in classical thermodynamics, and a general derivation of thermodynamic limits from the first and second laws of thermodynamics. In Section 3, I will then describe how thermodynamics constrains Earth system processes directly or indirectly by describing applications to atmospheric motion, hydrologic cycling, and the productivity of the terrestrial biosphere. For each of the examples, I will first describe the examples in thermodynamic terms, describe how they relate to optimality, derive simple estimates, link these
80 to established concepts in their respective fields, and then relate these examples back to the general picture shown in Figure 1. In Section 4 I then describe some of the limitations and potential future extensions, place previously proposed thermodynamic optimality approaches into the thermodynamic Earth system view described here and discuss potential applications of this approach to do simple, physics-based Earth system science. I close with a brief summary and conclusions.

2 Thermodynamics and Earth system functioning: What's missing?

85 All energy conversions within the Earth system are governed by the laws of thermodynamics. The first law of thermodynamics states that energy is overall conserved when it is converted from one form into another, while the second law requires that entropy can only remain the same or increase when energy is converted. Taken together, these laws set the limit to how much work can at best be derived from an energy source. A state of maximum entropy defines a reference point in thermodynamics, which corresponds to a state of thermodynamic equilibrium, a state from which no work can be derived. All of this is well-
90 established textbook knowledge.

So which components are missing when we want to apply thermodynamics and optimality to Earth system science? In this section, I describe a few components that are less commonly known but essential for describing a full picture of the Earth as a thermodynamic system: This includes more general definitions of entropy and free energy that goes beyond heat, a more general derivation of limits that goes beyond thermodynamic cycles and is solely based on the laws of thermodynamics, and
95 the inclusion of interactions with the boundary conditions in that limit. Historically, the laws of thermodynamics developed in the 19th century around the time of steam engines and the onset of industrialisation, focusing on the energy conversions related to heat, or thermal energy, and mechanical work. Boltzmann's statistical interpretation of entropy in the latter part of the 19th century formed the basis to extend the concept of entropy to other forms of energy beyond heat, prominently reflected in Planck's theoretical derivation of the radiation laws. This, in turn, has led to the revolution of quantum physics at
100 the onset of the 20th century. This has generalised the applicability of the laws of thermodynamics beyond the conversions of heat into mechanical work to all forms of conversion of energy into work. This is relevant to the Earth system because its primary forcing, solar radiation, is an energy source of very low entropy that does not come in form of heat, but in form of

electromagnetic waves. This is captured by the entropy of radiation, rather than heat, a concept that, while well established, is much less present in common climatology textbooks. Hence, the notion of entropy and the laws of thermodynamics apply to

105 far more energy conversions than simply to the conversion of heat into mechanical work (in fact, it would therefore be more appropriate to refer to the *energetics* of the Earth system, rather than its *thermodynamics*).

The question of how dynamics then form in the Earth system relates primarily to how work can be derived from the solar forcing. The solar forcing represents an energy source of very low entropy, as it is in thermodynamic disequilibrium with the thermal conditions of the Earth system. From this disequilibrium, work is derived, which sustains the dynamics of Earth

110 system processes, before this energy is dissipated and degrades to higher entropy. Essentially all Earth system processes, such as atmospheric motion, flows and transport processes, chemical transformations, metabolic activities, and socioeconomic activities of human societies, are sustained by work being done and reflect thermodynamic disequilibrium in different forms. Interior processes perform work, but with much lower magnitude, so that they are omitted here (but see, e.g., Dyke et al., 2011, for an application). Thermodynamics and optimality of Earth system processes thus relates intimately to the question of how

115 much work can be derived from the solar forcing.

In the following, the concepts just described are provided in greater detail, as these are typically not treated in textbooks of classical thermodynamics and of Earth system science. The description is aimed at a general level for a broader readership. For a fuller and more detailed description, the reader may be referred to textbooks in non-equilibrium thermodynamics (Kondepudi and Prigogine, 1998), literature on radiation entropy (Landsberg and Tonge, 1979; Kabelac, 1994; Wu and Liu, 2010), or the

120 application of these concepts to Earth system science (Kleidon, 2016).

2.1 Three forms of entropy

Entropy is one of the key concepts in thermodynamics. It is very well defined in statistical physics, which extends far beyond the much narrower use of entropy in classical thermodynamics, based on Clausius' expression of a change in entropy being caused by the change in heat content divided by its temperature. It originates from the quantization of energy at the microscopic scale

125 of atoms and molecules. At this scale, energy comes in discrete amounts called quanta, which are distributed over a discrete number of quantum states. This recognition, introduced by Boltzmann and Planck, led to the revolution in physics at the onset of the 20th century and amounted in the development of quantum physics.

Yet, when we deal with physical variables that characterize Earth system processes, such as temperature, pressure, density, relative humidity, concentrations or wind speeds, these refer to characteristics at the macroscopic scale of solids, liquids and

130 gases. At this scale, we do not want to deal with the details of how energy quanta are distributed at the microscopic scale. Hence, we need a scaling approach to map relevant aspects of how energy is distributed at the microscopic scale to the macroscale. This is where entropy comes into play (Figure 2).

Formally, entropy is defined as the probability of distributing a given amount of energy (hence, a certain number of quanta) over a certain number of quantum states. Since both are discrete, they can be counted, and hence this defines a probability.

135 This is where Boltzmann's famous equation, $S = k_b \log W$, comes into play: entropy S is directly proportional to the logarithm of this probability W, with the proportionality described by the Boltzmann constant, k_b, a fundamental constant in physics.
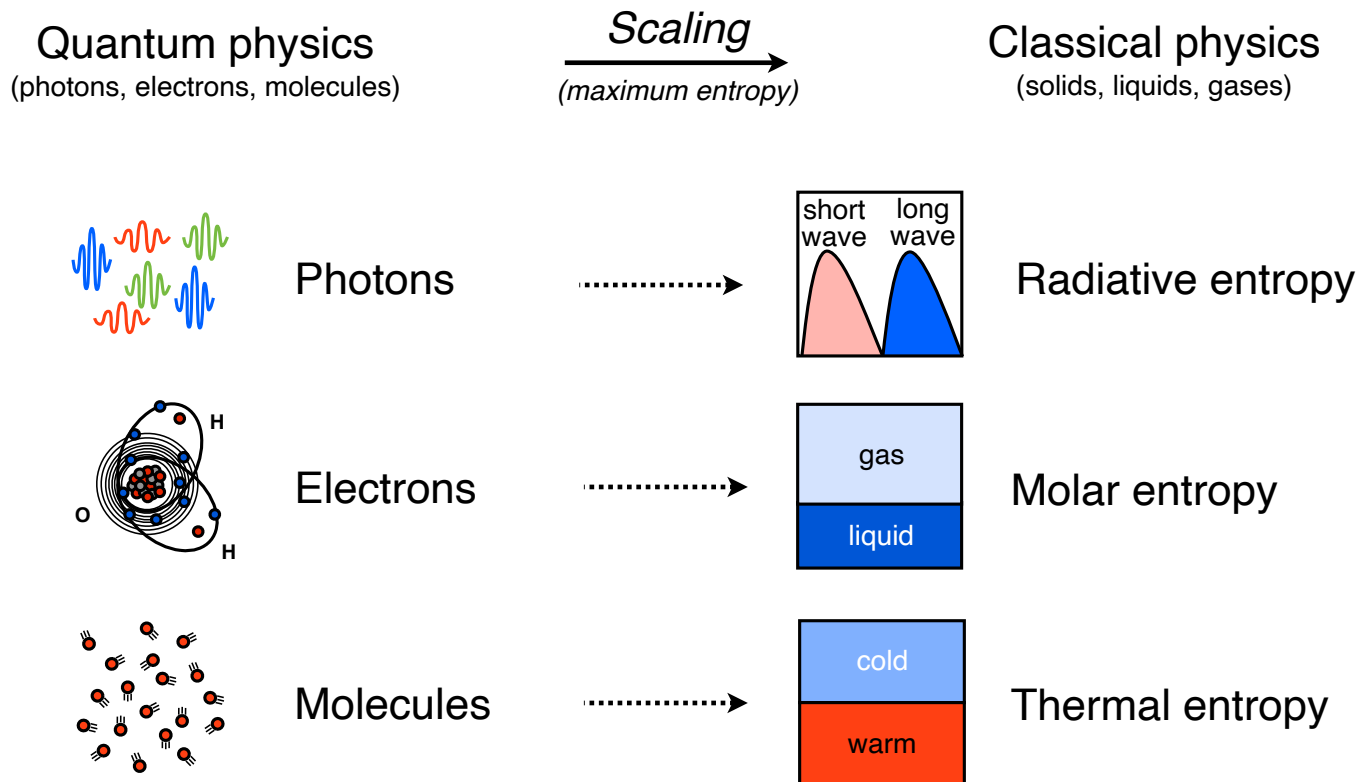
Figure 2. Energy is quantized and distributed over a discrete number of states at the scale of atoms and molecules (left). The associated scaling to variables in classical physics (right) is done by assuming maximum entropy. Depending on where the energy is stored at the microscopic scale, there are three different forms of entropy, associated with energy being distributed over photons, electrons, and molecules.

The state of thermodynamic equilibrium is then the state with maximum entropy, which simply means the most probable distribution of energy at the microscopic scale. From this state of maximum entropy, macroscopic variables such as temperature or pressure can then be derived. Note that Boltzmann's expression is sometimes also used to define information entropy. This concept, however, does not relate to the distribution of energy at the microscopic scale of quantum physics and is outside the scope of this paper.

A critical point to recognize is that when we deal with Earth system processes, we deal with processes that distribute energy quanta across radiation, matter, and random molecular motion. At the microscopic scale, these refer to different quantum states, with quanta of energy being distributed either over photons of different frequencies, different energy levels of electrons in atoms and molecules, and different vibrational, rotational or translational modes of molecules. Hence, this results in three different forms of entropy (Figure 2): radiation entropy, molar entropy, and the more common form of thermal entropy. These three forms of entropy are associated with the different distribution functions in statistical physics: the Bose-Einstein statistics for photons, the Fermi-Dirac statistics for electrons, and the Maxwell-Boltzmann statistics for random molecular motion.

This distinction between different forms of entropy is hidden in assumptions that are implicitly made when describing
150 the conversion of the energy contained in solar radiation by Earth system processes (as illustrated in Figure 1). When solar
radiation is absorbed and heats the surface, it is not just the energy that changes its form from radiative to thermal energy.
Also, the entropy changes its form. The second law of thermodynamics nevertheless applies. We usually do not recognize
these changes in forms, because commonly, local thermodynamic equilibrium is being assumed during the conversion. When
the Stefan-Boltzmann law is used to calculate the emission of radiation from a surface, it implicitly assumes thermodynamic
155 equilibrium between the kinetic temperature of the surface associated with random vibrations and motion of molecules and the
spectral composition of the emitted radiation.

The relevance of this distinction becomes clearer when we focus on how much work can be derived from converting solar
radiation. There, it makes a substantial difference if solar radiation is first turned into heat after it has been absorbed and then
turned into work (as is the case for a heat engine), or if it is used to change electronic states in photochemical or photovoltaic
160 conversions, generates chemical or electric energy before it eventually turns into heat (as are the cases for photosynthesis and
human-made photovoltaic technology). The latter conversions can derive substantially more work from the solar energy source
than the former. We will get back to this important difference further below.

2.2 From energy to free energy

The ability to perform work is closely connected to the term free energy. Free energy is commonly associated with a somewhat
165 narrower definition and specific expressions in thermodynamics, such as those for the Helmholtz or Gibbs free energy. Yet,
when we think of it more broadly, it refers to energy that resulted from work being performed. Examples within the Earth
system include the work done by acceleration to maintain motion against friction and the work of lifting water vapor against
gravity that maintains hydrologic cycling. This work results in free energy being generated, which can then be converted freely
into other forms. In the two examples, free energy is the kinetic energy of motion and the potential energy of water at a certain
170 height.

A more general definition for free energy is that it represents the fraction of energy at the macroscopic scale that has no
entropy associated with it. It is generated from work (or power, being equal to work over time), using an energy source of low
entropy, it can be converted further into other forms, and it can be dissipated, that is, converted back into heat (or radiation),
with a certain entropy that is typically higher (Figure 3). For instance, the kinetic energy of the atmosphere is generated out
175 of differential radiative heating and cooling at different temperatures, which represent energy sources and sinks of different
entropies. The free energy is dissipated by friction back into heat at a certain temperature, thus it gains a certain entropy again,
or it is converted further into other forms of free energy, for instance, by generating waves at the ocean surface or generating
electricity when used by wind turbines. Ultimately, these converted forms of energy eventually end up as heat (or radiation) as
well. At the end, the energy is emitted into space in form of terrestrial radiation, with a certain, higher radiative entropy.
180 Free energy budgets are central to describe the dynamics of Earth system processes. Atmospheric dynamics are about free
energy in kinetic form. Hydrologic cycling is about free energy in potential form associated with water at a certain height,
which can then be converted into the kinetic energy of falling raindrops or into horizontal river flow once it rained down on
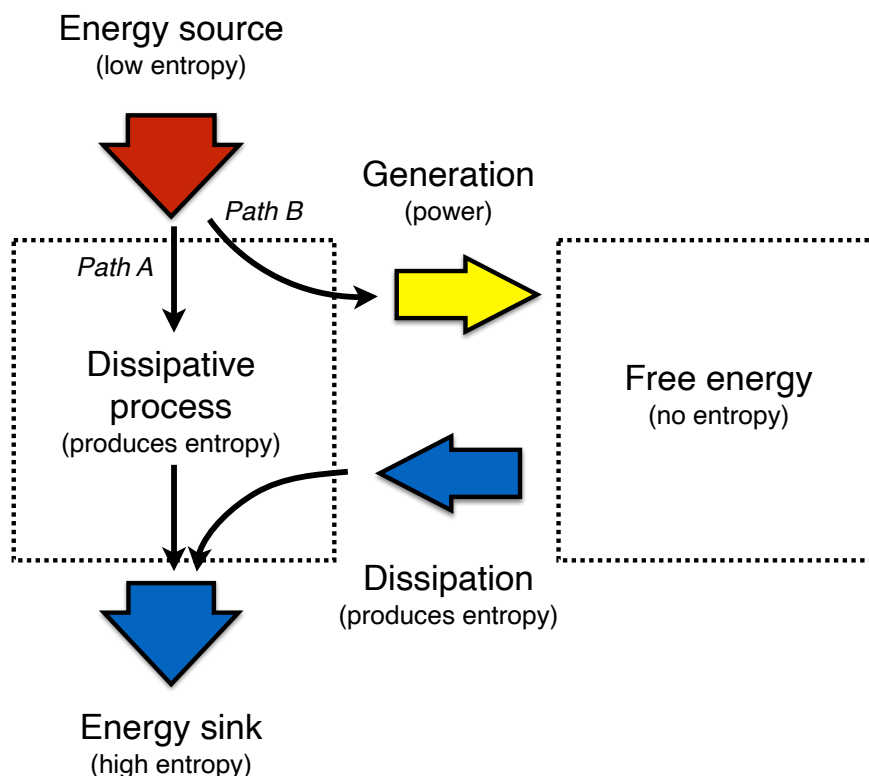
Figure 3. Free energy is generated by work being performed (or power, work over time) from an energy source with low entropy. This energy can then be further converted or dissipated back into a form of energy with entropy, typically of higher entropy. This distinction of free energy allows us to differentiate processes that merely dissipate and produce entropy, such as diffusion or radiative transfer (labeled as "Path A"), from those that involve free energy and macroscopic dynamics, such as atmospheric motion (labeled as "Path B").

land. The dynamics of ecosystems are about free energy in chemical form associated with the carbohydrates that make up biomass. These all can be formulated in terms of free energy budgets, a concept that is rarely used in Earth system science, but

185 that has the potential to provide a unified description because we deal with comparable processes and quantities, and processes where thermodynamics imposes restrictions on the magnitude of the conversions. These budgets are very different from energy budgets commonly used in climatology. Those merely deal with the accounting of heating and cooling terms in the budgeting of thermal energy.

Note that in some engineering literature, the term exergy (e.g., Petela, 1964; Bejan, 2002; Rosen and Scott, 2003; Herrmann,

190 2006; Tailleux, 2013) is being used for free energy, which has essentially the same meaning as free energy used here. This use of free energy described here is also consistent with the more common notions of Gibbs (or Helmholtz) free energy, except that we focus here on the difference of the actual Gibbs free energy to its respective minimum. The definition of free energy as energy without entropy becomes clearer and intuitive when we derive the limit to free energy generation in the next section.

We can now link these free energy dynamics back to the more general thermodynamic concepts of disequilibrium and
195 entropy production. When free energy is available, it means that it can be converted back into heat, so it has entropy attached to
it. That is, free energy within a system represents thermodynamic disequilibrium because when it is dissipated, the added heat
results in an increase in entropy in the system. Hence, the dissipative terms of the free energy dynamics are closely associated
with the intensity of entropy production that are due to the dynamics within a system. Yet, when focusing only at entropy
production, one cannot distinguish whether this entropy was produced by dynamics that involves free energy (such as motion,
200 labeled "Path B" in Figure 3) or not (such as diffusion or radiative transfer, labeled "Path A" in Figure 3). We will see that
this distinction is relevant when exploring thermodynamic optimality principles because it will allow us to understand why and
how a system may evolve to a thermodynamically optimal state.

2.3 Limits on generating free energy

When we now ask how much free energy can at best be derived for a certain energy source, the laws of thermodynamics set a
205 firm upper limit. The most common limit is the Carnot limit of a heat engine, that is, the limit of how much work, or free energy,
can be derived from a heating source. In textbooks, this limit is typically derived for a specific, so-called thermodynamic cycle,
involving different steps of expansion and compression. However, the Carnot limit can, in fact, be derived more generally and
more directly from the first and second laws of thermodynamics in a few steps, also for a flux-driven system in disequilibrium,
and also for energy sources other than heat.
210 The starting point is the first law of thermodynamics. We consider an energy conversion process, such as a conventional
power plant (Figure 4). This power plant generates heat by combustion of the chemical free energy stored in fossil fuels at a
rate J_{in}, it converts some of it into electricity at a rate G (or motion, in case of the internal combustion engine), while another
part, the so-called waste heat flux, J_{out}, leaves the power plant, as can be seen by the plumes emerging from the cooling towers.
The first law requires that in steady state with no changes in heat content, these energy fluxes are in balance, so that:

215 $$J_{in} = J_{out} + G \tag{1}$$

Note that G, the generation rate of electricity, represents the continuous work performed by the system, that is, its power.
The second ingredient shaping the upper limit on energy conversion comes from the entropy budget of the system and
the requirement imposed by the second law. When heat is added to the system, it is added with a certain temperature, T_{in},
which increases the entropy of the system at a rate J_{in}/T_{in}. The waste heat flux removes heat at a different temperature, T_{out},
220 so it reduces the entropy of the system at a rate J_{out}/T_{out}. The heat fluxes thus accomplish the entropy exchange with the
surroundings. We consider a steady state (as in Eq. 1), so we have no changes in heat storage within the system, and hence, no
change in entropy of the system in time. The difference between these two entropy exchange fluxes is balanced by the entropy
production, σ, within the system, so that our entropy budget in steady state is represented by

$$\frac{J_{in}}{T_{in}} = \sigma + \frac{J_{out}}{T_{out}} \tag{2}$$
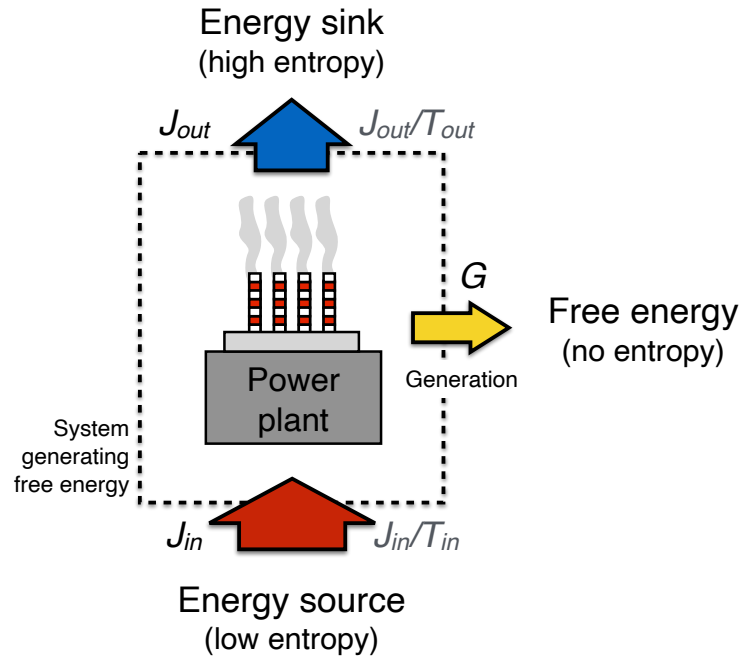
Figure 4. The first and second law of thermodynamics set the upper limit ("Carnot limit") on performing work and generating free energy, here illustrated using a "power plant" as an example. The first law requires that in the process of generating free energy, G, the fluxes (symbols in black) in, J_{in}, and out, J_{out}, of the generating system are balanced, so that $J_{in} = J_{out} + G$. The second law requires that the entropy flux out of the system (J_{out}/T_{out}, in grey) is greater or equal to the entropy flux into the system (J_{in}/T_{in}). At the Carnot limit, the entropy fluxes in and out of the system balance each other, yielding the greatest generation rate G.

225   Note that the generation rate G is not a part of the entropy budget because it generates free energy, that is, energy without entropy attached to it (as described in Section 2.2 above). To fulfill the requirement of the second law, the entropy production in Eq. 2 can only be $\sigma \geq 0$.

In the best case, $\sigma = 0$, so no entropy is being produced by this conversion process. Then, Eq. 2 simply yields $J_{out} = J_{in} \cdot T_{out}/T_{in}$, which can be combined with Eq. 1 to yield the limit of how much free energy can at best be generated:

$$230 \quad G = J_{in} \cdot \frac{T_{in} - T_{out}}{T_{in}} \tag{3}$$

This expression is known as the Carnot limit. It states that only a fraction $(T_{in} - T_{out})/T_{in}$, known as the Carnot efficiency, can at best be converted from the heat flux J_{in} from the energy source into power G.

This derivation of the Carnot limit is general and quite different to common textbook derivations, as it makes no specific assumptions about how this conversion process actually looks like. It includes merely the fluxes and conditions of the surround-
235   ings, and the two laws of thermodynamics. It is also general because instead of heat, one could use the same steps to derive an

equivalent limit for the direct conversion of radiation into free energy (without heat being involved in the conversion), as it has been done to derive limits for photosynthesis and photovoltaics (Press, 1976; Landsberg and Tonge, 1979, 1980).

When we place such a conversion process into the Earth system, we also need to account for the fact that eventually, the generated free energy is dissipated back into heat. That is, in steady state where there is no change of free energy in time, the

240 free energy budget is given by $G = D$. The dissipated heat is added back to the system. In principle, we can think of two cases where this heat is added: (i) it is added at the warm side where heat enters the generation process, so it would contribute to J_{in}, or (ii) it is added at the cold side where it contributes to the waste heat flux J_{out} that cools the system. As can easily be shown, the second case yields the same limit as Eq. 3, while the first case yields a slightly different limit where the temperature in the denominator is replaced by T_{out}. This limit has been referred to as the limit of a so-called dissipative heat engine (Renno and

245 Ingersoll, 1996; Bister and Emanuel, 1998), and yields slightly more power in applications to atmospheric science than Eq. 2 because $T_{out} < T_{in}$.

Looking at free energy generation yields a more differentiated view than just looking at entropy production, as has been done in applications of the proposed MEP hypothesis. We can see this by evaluating the entropy budget of the whole system that includes generation and dissipation of free energy. This system produces entropy by the dissipation, with its rate given

250 by the steady-state condition $G = D$. When we use the Carnot limit for G and assume that the dissipation takes place at the temperature T_{out}, we obtain for the entropy production σ:

$$\sigma = \frac{D}{T_{out}} = \frac{G}{T_{out}} = J_{in} \cdot \frac{T_{in} - T_{out}}{T_{in} T_{out}} = \frac{J_{in}}{T_{out}} - \frac{J_{in}}{T_{in}} \tag{4}$$

In other words, the entropy production of the system is entirely determined by the heat fluxes and the temperatures at the boundaries of the system, but it does not depend on whether the system generates free energy or not.

255 This points out another deficit when looking at a system only in terms of its entropy production: We cannot distinguish the case in which a system is so inefficient that it does not generate any free energy from the opposite case in which a system generates free energy at the Carnot limit and shows the strongest dynamics allowed for by the laws of thermodynamics. In the first case, all entropy production results from diffusion-like processes such as heat diffusion or radiative transfer, while in the second case, all entropy production results from dynamics that involve the generation and dissipation of free energy. When

260 we aim to understand a habitable planet like Earth, this distinction is critical – after all, the planetary role of life is fuelled by the free energy it generates and the work it does in chemically transforming its environment, and not by entropy production in general.

2.4 Interacting boundary conditions and the maximum power limit

When we want to apply thermodynamic limits to the Earth system, we need to recognise that the boundary conditions are often

265 not fixed, but react to the dynamics within the system that result from the generated free energy. This is a different situation compared to typical cases in classical thermodynamics where the boundary conditions of a system are fixed. In the Earth system, the only aspect that is truly fixed is the rate of incoming solar radiation at the top of the atmosphere. This lack of fixed
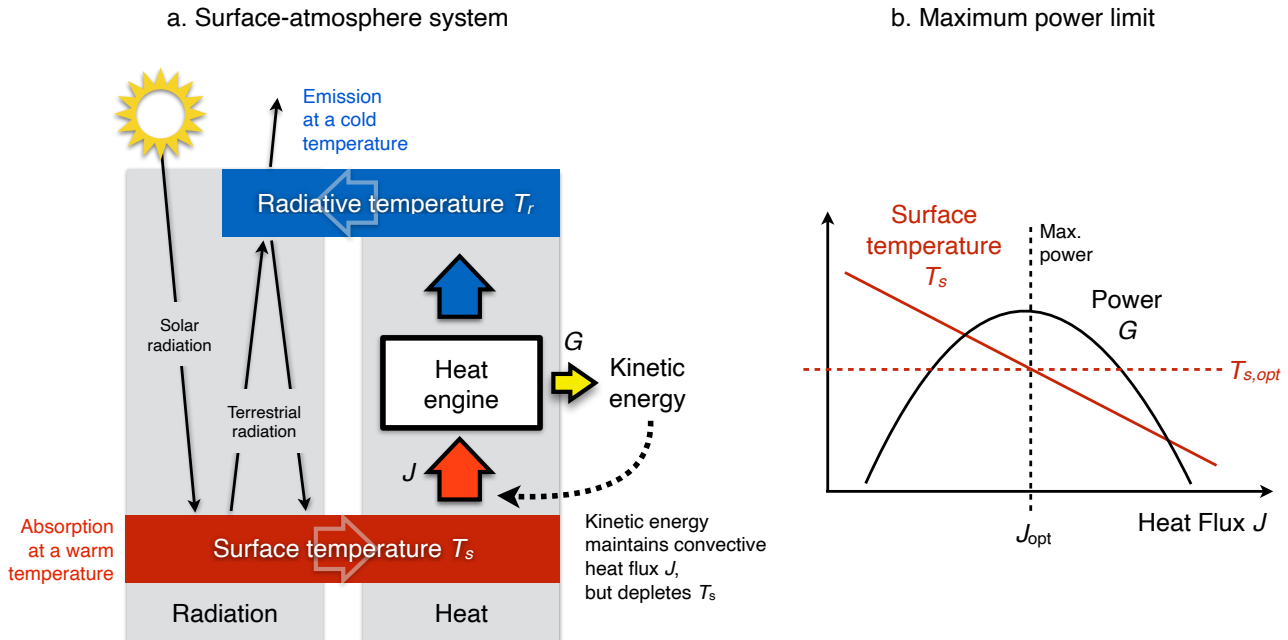
Figure 5. a. Schematic diagram of the energy balances of the surface-atmosphere system that set the boundary conditions for the operation of an atmospheric heat engine that generates vertical convective motion. This engine generates kinetic energy associated with atmospheric convection, which transports heat from the surface into the atmosphere, thereby lowering the temperature difference between the surface and the atmosphere. b. The trade-off between a greater heat flux resulting in a colder temperature results in a maximum power limit for the heat engine, an optimum sustained level of turbulent heat fluxes J_{opt} for surface-atmosphere exchange and an associated, optimum surface temperature $T_{s,opt}$. After Kleidon and Renner (2013a).

boundary conditions is particularly relevant for those cases where free energy is generated and the resulting dynamics alters these boundary conditions.

270   This is the case for the surface-atmosphere system (Figure 5), where the absorption of solar radiation heats the surface, emission of radiation cools the atmosphere, resulting in a differential heating of the surface-atmosphere system. This differential heating is used to perform the work to generate convective motion, this motion transports heat, and this heat transport depletes the radiative heating difference. This results in a lower temperature difference, thereby affecting the boundary conditions. Mathematically, this is represented by a dependence of the second term (the efficiency term) on the heat flux in the Carnot

275   limit (cf. Eq. 3). This interaction can easily be accounted for and leads to a maximum power limit. The maximum power limit has been recognised widely, for instance, in electrical engineering and in some relevant literature concerning the Earth system (Lotka, 1922a, b; Odum and Pinkerton, 1955), but typically not in thermodynamics.

In the following, I want to use convective motion in the surface-atmosphere system as an example to illustrate that these interactions can easily be accounted for by formulating the associated energy balances. These energy balances determine the

280   temperature difference that drives the generation process of the heat engine, but are affected by the heat flux that is associated

with the convective motion that is being generated. In other words, we consider atmospheric convection as being the result of

an atmospheric heat engine that operates from the differential radiative heating, with solar radiation heating the surface, and

thermal emission to space cooling the atmosphere (as described in Kleidon and Renner (2013a)).

     To start, we consider two energy balances to describe the system (Figure 5): (i) the surface energy balance, where most

285   of the solar radiation is absorbed and from which the surface temperature T_s can be inferred from the emission of terrestrial

radiation, and (ii) the energy balance of the whole system, which balances total absorption of solar radiation with total emission

of terrestrial radiation to space, which sets the radiative temperature T_r.

     The surface energy balance consists of the absorption of solar radiation, R_s, and downwelling terrestrial radiation, $R_{l,down}$,

both of which heat the surface (i.e., a conversion of radiative into thermal energy), and the cooling by emission of radiation

290   (i.e., a conversion of thermal into radiative energy) as well as a heat flux J that results from the generation of vertical motion

(the sensible and latent heat flux, combined here for simplicity):

$$R_s + R_{l,down} = \sigma T_s^4 + J \tag{5}$$

     Here, we assume that the surface emits like a blackbody, with σ being the Stefan-Boltzmann constant ($\sigma = 5.67 \cdot 10^{-8}$ W

m^{-2} K^{-4}). We further neglect changes in heat storage or net horizontal transport of heat, which can be relevant for ocean

295   surfaces.

     The energy balance of the whole system is set by the total absorbed solar radiation, $R_{s,tot}$, and the emission of terrestrial

radiation to space:

$$R_{s,tot} = \sigma T_r^4 \tag{6}$$

     where T_r denotes the radiative temperature. The use of the radiative temperature here has a thermodynamic motivation:

300   Since blackbody radiation is radiation at maximum entropy, the radiative temperature is the lowest temperature at which the

absorbed solar radiation can be emitted to space, representing the highest radiative entropy export from the Earth system. It

is thus the coldest temperature from which work can be derived in a climatological mean setting, and yields the upper bound

on how much power can maximally be derived. Note that this temperature is not the temperature of a specific height within

the atmosphere, but entirely focused on the most optimistic entropy export associated with the emission of outgoing longwave

305   radiation.

     With these energy balances, we have a formulation of the two temperatures, T_s and T_r, and can evaluate the maximum power

that can be derived from the Carnot limit (Eq. 3). When we consider a greater J, then T_s decreases according to the surface

energy balance (Eq. 5), while T_r remains unaffected. A greater J thus results in a depleted temperature difference $T_s - T_r$

and a lower efficiency term in the Carnot limit. As a result, the power derived from the heat flux has a maximum (a maximum
310 power limit), which is achieved with an intermediate, optimum value of the heat flux of

$$J_{opt} = \frac{1}{2} \cdot (R_s + R_{l,down} - R_{l,0}) \tag{7}$$

where $R_{l,0}$ is a constant term that originates when the Stefan-Boltzmann law is linearized in the form $R_{l,up}(T) = R_{l,0} + k_r(T - T_0)$ for simplicity (with T_0 being a fixed reference temperature, $R_{l,0} = \sigma T_0^4$ and $k_r = 4\sigma T_0^3$ is the linearisation constant). The surface temperature associated with this maximum in power is then given by

$$315 \quad T_s = T_r + \frac{R_s + R_{l,down} - R_{l,0}}{2k_r} \tag{8}$$

In other words, the maximization of power constrains the dynamics such that the magnitude of the heat flux J as well as the resulting surface temperature T_s can be predicted from it. The outcome then only depends on the radiative forcing and certain assumptions pertaining to how radiative transfer is formulated (e.g., the height of convection, Dhara et al. (2016); or the longwave optical thickness, Conte et al. (2019)).

320 This maximum power limit results from this lack of fixed boundary conditions at the surface. Yet, the interaction that is caused by the response of the surface temperature to varying magnitudes of the heat flux J is nevertheless constrained by the response of the surface energy balance and can thus be accounted for. As we will see further below, this maximum power limit plays a highly relevant role as it can explain observed surface energy balance partitioning and associated evaporation rates very well, implying that this limit does not just exist, but that atmospheric motion apparently evolves to and operates at this
325 limit. As it only contains energy balances and the assumption of convective motion operating at the maximum power limit of free energy generation, it would seem that this limit can explain much of the emergent simplicity observed in climatological patterns (which we will look at further below).

2.5 Putting things together

At the end of this section let us quickly sum up the main concepts of this section and what these imply for thermodynamics
330 and optimality in the Earth system (Figure 6).

The three forms of entropy are at play when we follow the energy conversions within the Earth system. The energy source of solar radiation is energy in form of a flux of electromagnetic radiation with short wavelengths, representing low radiative entropy because solar radiation was emitted at a very high temperature. When it turns into heat upon absorption, it is converted into thermal energy with associated thermal entropy. When solar radiation is used by photosynthesis or photovoltaics, some
335 of the energy is converted into non-thermal forms of energy and molar entropy, but not heat. After being converted by Earth system processes, energy is eventually emitted to space in form of terrestrial radiation at much longer wavelengths, representing much higher radiative entropy because it was emitted at a much colder temperature than the Sun. So, clearly, this distinction of the three different forms of entropy plays a central role in Earth system processes, and it is important to distinguish these as well as the associated forms of energy.
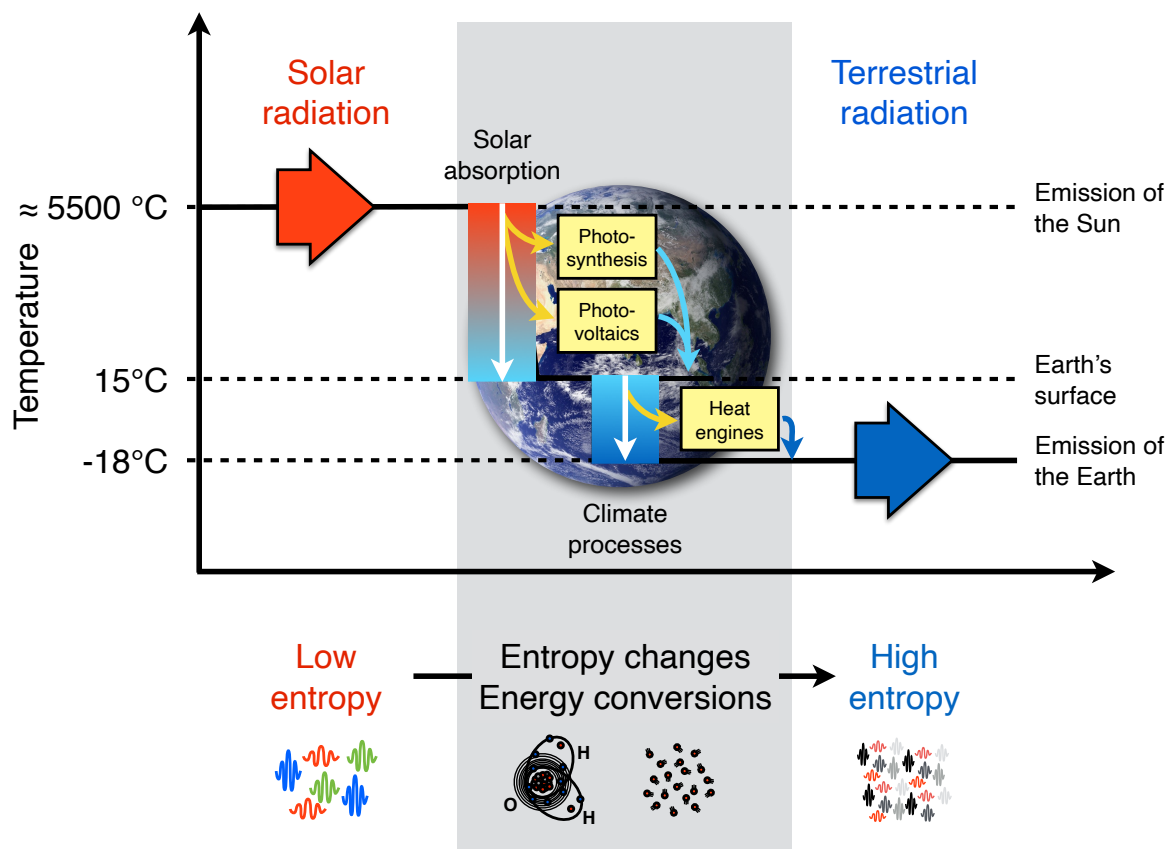
Figure 6. Energy is degraded and entropy is increased as solar radiation is converted into different forms of energy and entropy by Earth system processes, following the second law of thermodynamics. Physical processes derive their free energy from heat engines that are primarily driven by the temperature difference between the Earth's surface and the radiative temperature, while photosynthesis and photovoltaics generate free energy directly from solar radiation before it is converted into heat (yellow boxes). Thermodynamics limits how much free energy can at best be derived from these generation processes, thus constraining the resulting planetary dynamics.

340   Free energy is generated from solar radiation mainly by three different processes, as shown by the yellow boxes in Figures 1 and 6. The free energy contained in atmospheric motion in form of kinetic energy is generated by heat engines that operate equivalently to the example of the power plant used in the derivation of the Carnot limit (Eq. 3). Photosynthesis generates chemical free energy contained in carbohydrates and oxygen, while photovoltaics produces electric free energy (although currently at a much lower magnitude than photosynthesis). This free energy is associated with dynamics - like atmospheric
345   motion or metabolic activities of living organisms - and it can be converted further into other forms of free energy, e.g., associated with hydrologic (or other geochemical) cycling, ocean dynamics, trophic networks in ecosystems, or food production in human societies. Thus, by evaluating the magnitudes of these free energy generation processes at the beginning of energy

conversion chains starting with the conversion of solar radiation, we gain a general understanding of how active the dynamics of the Earth system are in thermodynamic terms.

350   Thermodynamic limits and optimality then apply first and foremost to these three processes as these convert solar radiation into free energy, constraining the resulting dissipative dynamics by the energy input into the energy conversion sequences. This then leaves the question whether Earth system processes are constrained by thermodynamic limits, whether this is then associated with optimal functioning that maximizes the free energy generation for Earth system dynamics, and how much of these limits is then reflected in the emergent climatological patterns that we can observe.

355 3 Thermodynamic Optimality and Maximization: How does it apply to Earth system processes?

In the following, I support this thermodynamic Earth system view by showing that it can predict observed patterns very well. This demonstrates the relevance of thermodynamic limits, but also of the systems' perspective because many processes only relate indirectly to these limits. I use three examples: poleward heat transport by the atmospheric circulation, evaporation as a key component of hydrologic cycling, and terrestrial carbon uptake as a measure of vegetation activity. Each of these examples

360   has previously been described in terms of some form of thermodynamic optimality and maximisation. I first describe how each of the examples relate to thermodynamics, free energy and to the maximum power limit as described in the previous section. I then present "minimum" models, that is, models that contain as little empirical information as possible except for the bare essential physics, to derive estimates for each example that relate to the maximum power limit. I do so with the objective to illustrate that the latter two cases do not follow the simple "flux depletes difference" scheme that is at the core

365   of the maximum power limit (as shown in Section 2.4 above). For these cases, one needs to explicitly consider the intimate connections among processes within the Earth system, particularly regarding transport limitations, so that they are indirect consequences of maximising power.

I will specifically use models that are as simple as possible to describe these examples. The motivation for this simplicity in formulation is to provide transparency and accessibility to the reader, and to not obscure outcomes with complex mathematical

370   formulations. Even at this simplest level, the outcomes will show the great importance of thermodynamic constraints because the derived estimates compare very well with observations. One can easily make these models more complicated, include more phenomena and parameterisations, or add greater spatial and temporal resolution, and achieve a better fit with observations. Yet, the thermodynamic constraint will still play out in more or less the same, although in a less transparent way.

With this reinterpretation of each of these examples, I will then discuss the linkages to previous interpretations of thermody-

375   namic optimality, specifically the proposed MEP hypothesis, and to established theoretical concepts.

3.1   Poleward heat transport and the large-scale atmospheric circulation

At its very core, the large-scale atmospheric circulation involves energy conversions as work needs to be done to maintain motion against friction. This work is derived from the difference in radiative heating between the warmer, equatorial regions and the colder, polar regions (Figure 7). Atmospheric motion involves free energy in form of kinetic energy, it transports

380 heat, thereby affecting the thermodynamic forcing, and the combination results in a maximum power limit, similar to the example in Section 2.4, but in the horizontal direction. We thus have a thermodynamic process which performs work by converting a heating difference into free energy, generates motion, which is dissipated back into heat due to friction and produces thermal entropy. Thermodynamic optimality has been applied to atmospheric motion in the past, most prominently in form of the proposed MEP hypothesis (starting with a series of papers by Paltridge 1975; 1978; 1979). Since maximizing

385 power also maximizes dissipation, and dissipation produces thermal entropy, it is easy to imagine that both maximizations result in roughly the same outcome. Power can also be related to the rate by which available potential energy is converted into kinetic energy, thus linking this thermodynamic approach to the more common theoretical concept of the Lorenz Energy Cycle (LEC, described by Edward Lorenz 1955; 1960; 1967). These linkages are described in more detail further below after we first describe a minimum model demonstrating the maximum power limit for the large-scale atmospheric circulation.

390 The maximum power limit for the large-scale circulation is demonstrated with a two-box model, in which we split up the Earth into two regions of same size at the $30°$ latitude to characterise the differential radiative heating from which the kinetic energy is being generated (as shown in Figure 7, as in Kleidon (2021a)). Due to the Earth's geometry, the tropical regions absorb more of the incoming solar radiation per unit surface area than the extratropical regions. This uneven heating results in a difference in surface temperatures between the tropics and the extratropics. As a result, the absorption of solar radiation in

395 the tropics adds more heat at lower entropy because it is absorbed at a higher temperature compared to the extratropics. The differential solar heating across latitudes thus sets the stage for an atmospheric heat engine, with the greater absorption of solar radiation in the tropics than the extratropics as the heat source, and the greater emission into space than the absorbed solar radiation in the extratropics as the heat sink. This heat engine performs the work to generate large-scale atmospheric motion and the associated kinetic energy, and is constrained by the Carnot limit (Eq. 3).

400 We obtain the maximum power limit for this heat engine in an equivalent way as in Section 2.4, but for the large-scale atmospheric circulation, we use the poleward heat transport as the heat flux and the temperature difference between the two boxes for the efficiency term. To quantify this maximum, we need a formulation of the energy balances to express how the temperature difference in the Carnot limit is depleted by the poleward heat transport. These temperatures can be inferred from the respective energy balances of the two boxes, because the thermal emission to space at the top of the atmosphere, R_l,

405 depends on surface temperature. We write the two energy balances as

$$R_{s,t} = R_{l,t} + J \qquad R_{s,p} + J = R_{l,p} \qquad (9)$$

where I used the index t for the tropical box ($30°$S - $30°$N), the index p for the extratropical box (latitudes greater than $30°$), R_s for the total absorbed solar radiation, and J for the poleward heat transport.

We then infer surface temperatures from R_l by using the empirical parameterization of Budyko (1969):

410 $$R_l = a + b \cdot T_s \qquad (10)$$
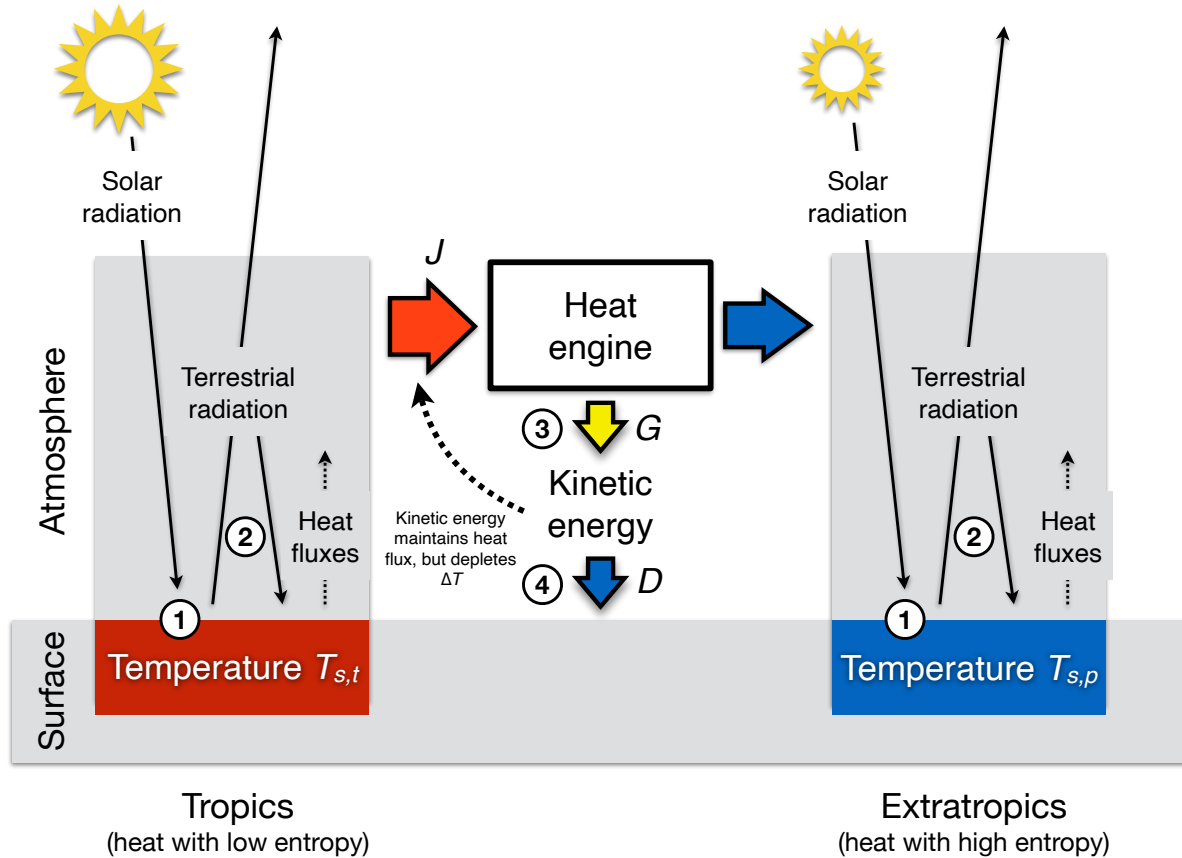
Figure 7. Schematic diagram of how kinetic energy is generated within the atmosphere by a heat engine that uses the difference in solar radiative heating between the tropics (left box) and the extratropics (right box) as a driver. The generated motion maintains the poleward heat transport J, but depletes the temperature difference $T_{s,t} - T_{s,p}$ between the two boxes. This results in a maximum power limit for the strength of the atmospheric generation. Also marked by the numbered circles are places at which thermodynamic conversions and entropy production take place: (1) conversion of solar radiation into thermal energy by absorption at the surface temperature, producing thermal entropy; (2) absorption of terrestrial radiation and re-emission as well as vertical, convective motions, which both produce thermal entropy; (3) generation of free energy from heat flux J; (4) frictional dissipation, that is, conversion of kinetic energy back into thermal energy, which produces thermal entropy.

where $a = -388.7\,\mathrm{W\,m^{-2}}$ and $b = 2.17\,\mathrm{W\,m^{-2}\,K^{-1}}$ are empirical constants, with T_s is in units of K. This linear relationship between surface temperature and the radiative flux to space compares very well to observations and can be explained by the role of water vapor in the atmosphere (Koll and Cronin, 2018).

When Eqns. 9 and 10 are combined, surface temperatures are functions of absorbed solar radiation and the poleward heat

415 flux J:

$$T_{s,t} = \frac{R_{s,t} - a - J}{b} \qquad T_{s,p} = \frac{R_{s,p} - a + J}{b} \tag{11}$$

Note how heat transport depletes the temperature difference due to the opposing signs in these two expressions. For a value of $J = 0$ in the absence of heat transport, temperatures are determined by the local solar radiative forcing only ($R_l = R_s$). This yields the largest temperature difference (Figure 8e), which would then yield the greatest efficiency in the Carnot limit. The

420 temperature difference vanishes with a value of $J_{max} = (R_{s,t} - R_{s,p})/2$, yielding a globally uniform surface temperature of $T_s = 290$ K and the efficiency in the Carnot limit vanishes to zero as well.

There is hence a maximum in the power at an intermediate value of J. It is obtained mathematically from the Carnot limit (Eq. 3), the temperature expressions (Eq. 11), an additional factor of 1/2 to account for the fact that heat is transported from one half of the Earth to the other, and then setting $dG/dJ = 0$ (see also Figure 8c). The slight dependence of the power on $T_{s,t}$ in the

425 denominator has been neglected here. This maximum yields a power of $G_{max} = (R_{s,t} - R_{s,p})^2/(16bT_{s,t})$, is associated with an optimum heat flux of $J_{opt} = (R_{s,t} - R_{s,p})/4$, which reduces the temperature difference $T_{s,t} - T_{s,p}$ to half of its maximum value in the absence of heat transport.

We next use the observed radiative forcing from the CERES radiation dataset (Loeb et al., 2018; Kato et al., 2018) to evaluate these expressions. The only information needed is the absorption of solar radiation for the two boxes. The observed flux of

430 terrestrial radiation serves as a means to test the outcome associated with the maximum power estimate. With climatological means of $R_{s,t} = 306$ W m^{-2} and $R_{s,p} = 177$ W m^{-2}, this yields a maximum in power to generate kinetic energy of 1.6 W m^{-2} (Figure 8c), which agrees quite well to the magnitude of kinetic energy generation of about 2.1 - 2.5 W m^{-2} inferred from the reanalyses (Li et al. 2007). The estimated value for the poleward heat transport of 32 W m^{-2} is a bit less than the 43 W m^{-2} diagnosed from the CERES dataset, resulting in a somewhat greater temperature difference of $T_{s,t} - T_{s,p} \approx 30$ K

435 compared to a value of 21 K derived from CERES. In other words, the maximum power limit predicts the magnitude of the free energy dynamics of the global atmosphere rather well, despite some discrepancies. This suggests that the atmosphere works as hard as it can to generate motion, and that its climatological characteristics can be adequately described by formulating the thermodynamic constraints in conjunction with energy budget, even in the simplest possible way as is done here.

This outcome of maximum power can be linked to the proposed MEP hypothesis and the more established LEC framework

440 of atmospheric energetics.

The link to the proposed MEP hypothesis is established by the thermal entropy production due to frictional dissipation, that is, when the free, kinetic energy is converted back into heat. In the climatological mean state, power balances dissipation, so that maximum power equals maximum frictional dissipation, which then is almost the same as maximised thermal entropy production due to frictional dissipation (Figure 8d). This entropy production term is what has been maximised in previous

445 applications of MEP to atmospheric heat transport. In other words, maximum power and MEP almost yield the same outcomes. Yet, we should recognise that the entropy production by frictional dissipation is only a tiny contribution to the overall entropy production of the planet (Figure 8b, see Appendix A for derivations), because absorption of radiation is typically associated with much greater rates of entropy production (Figure 8b) than that of frictional dissipation (Figure 8d). Focusing on maximum
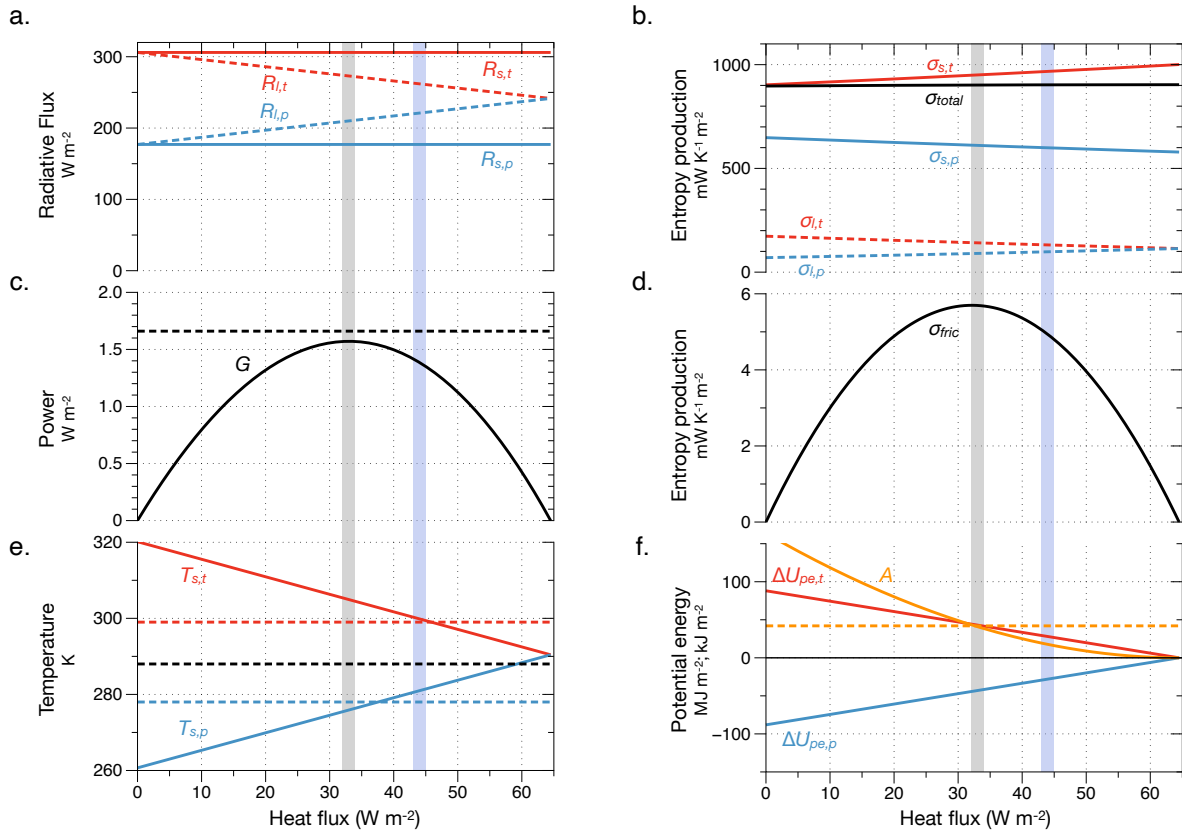
Figure 8. Radiative forcing and energetic properties estimated from the two-box model shown in Figure 7 relating to the strength of the atmospheric circulation and maximum power. a. Radiative forcing in terms of absorbed solar radiation ($R_{s,t}$ and $R_{l,t}$) of the tropical (red lines) and extratropical box (blue lines) and emitted terrestrial radiation to space ($R_{l,t}$ and $R_{l,p}$). b. Entropy production by absorption of solar radiation ($\sigma_{s,t}$ and $\sigma_{s,p}$, circles marked as (1) in Fig. 7), radiative transfer of terrestrial radiation ($\sigma_{l,t}$ and $\sigma_{l,p}$, (2) in Fig. 7), and total entropy production, σ_{total} (black line). c. Power G to generate atmospheric motion ((3) in Fig. 7). The horizontal dashed line marks the power inferred directly from the CERES forcing. d. Entropy production by frictional dissipation of kinetic energy ((4) in Fig. 7). e. Surface temperatures of the tropical (red line) and extratropical (blue line) boxes with the surface temperatures estimated from the CERES TOA flux marked by the dashed lines (black line: global average). f. Difference in potential energy compared to an isothermal Earth ($\Delta U_{pe,t}$, $\Delta U_{pe,p}$, in MJ m^{-2}, red and blue lines) and the available potential energy (A, in kJ m^{-2}, orange line, dashed orange line represents published estimates). The vertical shaded areas represent the value of heat transport from maximum power (grey) and inferred from the CERES data (blue). After Kleidon (2021a).

power rather than on MEP gives us a more specific view on which aspect of the system is maximised and why. After all, the

450   atmospheric circulation needs work to be maintained. Just focusing on entropy production, however, cannot distinguish between processes that involve work from those which do not, a point already made at the end of Section 2.3.

The link to the LEC is done by making the link between heating differences and kinetic energy generation more detailed by including the intermediate step of generating available potential energy (APE). Diabatic heating sources generate potential energy differences, from which only a fraction becomes APE, a concept originally introduced by Margules (1905). APE is then converted into kinetic energy (KE) at a certain rate. It is typically diagnosed from pressure and temperature fields of the atmosphere. The application of maximum power to atmospheric dynamics differs in that it takes the diabatic heating terms directly as the starting point, without the need for the intermediate step of APE generation. This can nevertheless be inferred from the conditions associated with the maximum power limit and compared to observations (Figure 8f, see Appendix B for derivations). The value of APE of $41 \cdot 10^5$ J m^{-2} associated with the maximum power limit matches the range of $40 - 50 \cdot 10^5$ J m^{-2} estimated from observations (Peixoto and Oort, 1992; Li et al., 2007) very well. Further conversions between APE and KE associated with the mean flow and eddies is generally considered as reversible within the LEC framework (which is inherent in the notion of geostrophic, frictionless flow), so that these conversions neither generate nor dissipate free energy. Thermodynamics and the maximum power limit therefore set a relevant constraint to the maximum intensity of the Lorenz Energy Cycle and it appears that the atmospheric circulation operates at this maximum.

To sum up, the large-scale atmospheric circulation provides an example for an Earth system process that maximises power from the large-scale differences in solar radiative heating. Even when applied to a simplest two-box model, it provides an estimate for the magnitude of poleward heat flux that broadly agrees with estimates derived from observations. Yet, the focus on power achieves more than focussing on the entropy production, because it provides us with an estimate of the strength of the dynamics - in terms of kinetic energy generation - and it allows us to link the thermodynamic view to the Lorenz Energy Cycle and its intensity. Hence, this case of maximum power does not contradict established theory, it rather adds a relevant constraint that is currently not acknowledged.

3.2 Evaporation and hydrologic cycling

At first sight, hydrologic cycling appears to primarily involve mass fluxes of water (Figure 9). Evaporation, the conversion of liquid water to vapor, takes place mostly at the surface, adding moisture to the atmosphere, while the opposite conversion takes place within the atmosphere, causes precipitation and removes moisture. In the climatological mean, both fluxes balance each other at the global scale. To understand how thermodynamics and maximum power constrain the magnitude of hydrologic cycling, we can thus either take a surface perspective and look at the factors that constrain evaporation, or an atmospheric perspective and look at precipitation.

Yet, hydrologic cycling is more than mass fluxes. At its core, it is a thermodynamic process which operates in a state of thermodynamic disequilibrium (Figure 9). Evaporation happens at warmer temperatures (circle (1) in Fig. 9), takes up latent heat, and changes thermal into molar entropy, while condensation occurs at colder temperatures, releasing this latent heat, converting molar into thermal entropy. Hydrologic cycling thus effectively transports heat from the warmer surface into the colder atmosphere, thereby producing thermal entropy.

Hydrologic cycling intimately involves work, free energy, and dissipation. Cloud droplets have potential energy that is generated by the work of lifting water, unsaturated air reflects the work done by dehumidification, and evaporation of seawater
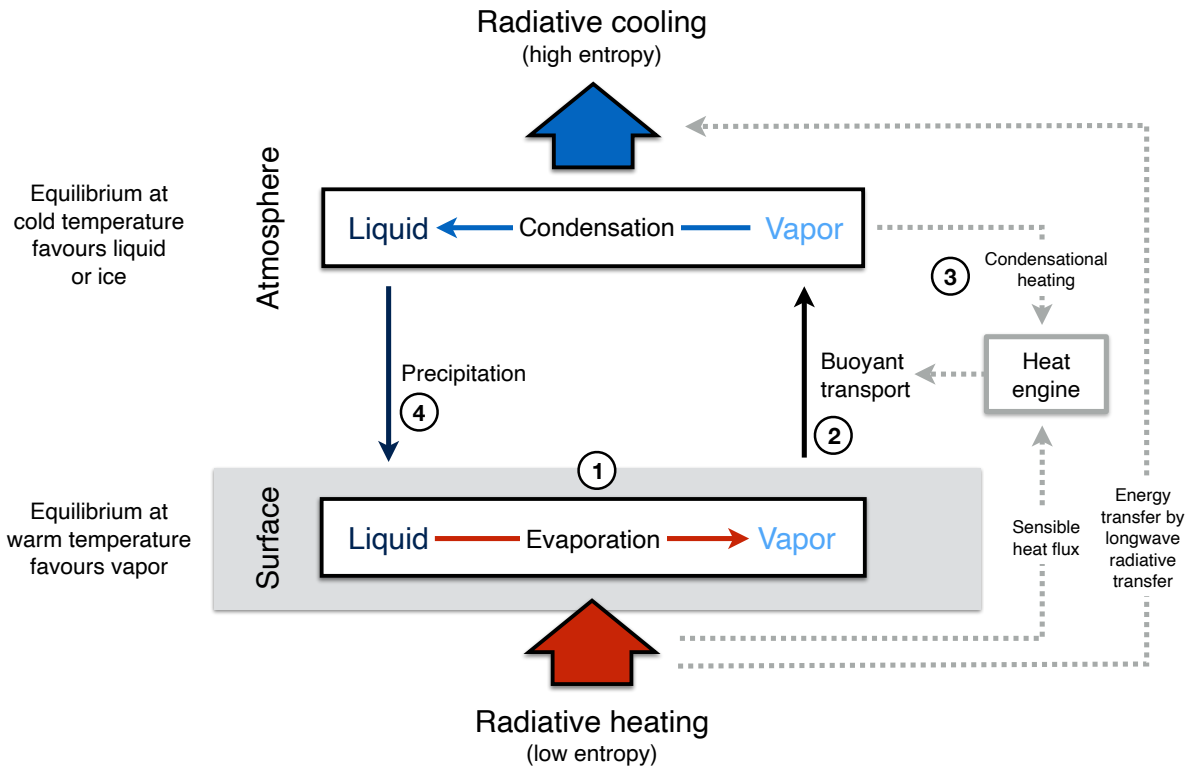
Figure 9. Thermodynamics of hydrologic cycling and its connections to the Earth system. The numbered circles mark places at which thermodynamic conversions and entropy production takes place: (1) Absorption of solar radiation heats the surface, and thereby shifts the thermodynamic equilibrium of a water surface towards higher saturation vapor, resulting in evaporation; (2) The saturated water vapor at the surface mixes with the unsaturated near-surface air, producing entropy; (3) Moist air is lifted until it condenses. The condensed heat drives a moist heat engine that generates kinetic energy for moist convection; (4) falling raindrops dissipate their potential energy that was generated by lifting moistened air, resulting in frictional dissipation and thermal entropy production. The link to the maximum power limit of vertical convection (Sect. 2.4) is made by noting that it requires the work of buoyancy to lift moisture up to the condensation level.

involves desalination work and the generation of chemical free energy. The potential energy of cloud droplets is dissipated as raindrops fall (circle (4) in Fig. 9), by gravitational drainage when the precipitated water reaches the land surface, or is converted into the kinetic energy of river flow. The chemical free energy in freshwater drives continental weathering processes that dissipate the disequilibrium between the desalinated rainwater and the solid minerals of the continental crust. So clearly,

490 thermodynamics and free energy are at the very core of hydrologic cycling, and it would appear that these can act to restrict its magnitude.

  How, then, do we relate hydrologic cycling to maximum power and infer optimal characteristics associated with this maximization? What I show here is that one can infer adequate magnitudes for evaporation from an indirect application of maximum power, indirect in that it does not involve maximizing the power of a hydrologic flux directly (e.g., the maximum power to lift

or to generate moist convection), but rather the maximum power of generating buoyant exchange and vertical transport from radiative heating of the surface, as described in Section 2.4. When solar radiation heats a surface at which water is sufficiently available, it adds sensible and latent heat to the near-surface air, making it warmer and moister. The upper, thermodynamic limit on moistening is set by adding saturated air, as this represents the thermodynamic equilibrium state. The associated equilibrium partitioning is well known in micrometeorology, was developed by Schmidt (1915), Penman (1948), and Slayter and McIlroy (1961), and is reflected in approaches to estimate potential evaporation, such as the well-known Priestley-Taylor estimate (Priestley and Taylor, 1972). This implies that thermodynamics and maximum power primarily constrain the magnitude of buoyant transport from the surface to the atmosphere, which combined with the thermodynamic equilibrium at the surface constrains the magnitude of evaporation and thus of hydrologic cycling.

To make this constraint more explicit, we first apply this equilibrium partitioning to the optimum heat flux, J_{opt}, derived from maximum power (Eq. 7). Over a short time interval dt, the near-surface air is simultaneously warmed by dT and moistened by an increase in saturation vapor pressure, $de_{sat} = s \cdot dT$, with $s = de_{sat}/dT$ given by the Clausius-Clapeyron equation (this reflects the upper limit of adding saturated air to the atmosphere). If we consider a small volume of this air, V, this addition results in contributions of warming, dU_H, of

$$dU_H = c_p \rho V \cdot dT \tag{12}$$

and moistening, dU_{LE}, of

$$dU_{LE} = L \cdot \frac{dq_{sat}}{dT} \cdot \rho V \cdot dT = L \cdot \frac{R_a}{R_v} \cdot \frac{1}{p} \cdot s \cdot \rho V \cdot dT \tag{13}$$

with c_p being the heat capacity of air ($c_p = 1005$ J kg^{-1} K^{-1}), ρ being air density ($\rho \approx 1.1$ kg m^{-3} for typical surface conditions), L being the latent heat of vaporization ($L \approx 2.5 \cdot 10^6$ J kg^{-1}), q_{sat} being the saturation specific humidity (with $q_{sat} = R_a/R_v \cdot e_{sat}/p$), R_v and R_a the ideal gas constants of water vapor and air (with $R_a/R_v \approx 0.622$), p the surface pressure ($p = 1013$ hPa for average surface conditions).

Since $dU = dU_H + dU_{LE}$, we can then derive the relative partitioning among heating and moistening at thermodynamic equilibrium, noting that the terms $\rho V \cdot dT$ cancel out while collecting the other constants in the so-called psychrometric constant $\gamma = c_p p (R_v/R_a)/L \approx 65$ Pa K^{-1}. The relative partitioning is then given by the ratios

$$\frac{dU_H}{dU} = \frac{\gamma}{s+\gamma} \qquad \frac{dU_{LE}}{dU} = \frac{s}{s+\gamma} \tag{14}$$

When combined with the optimum heat flux derived from maximum power, we obtain the following partitioning into sensible and latent heat

$$H_{opt} = \frac{\gamma}{s+\gamma} \cdot J_{opt} \qquad LE_{opt} = \frac{s}{s+\gamma} \cdot J_{opt} \tag{15}$$

a. Evaporation estimate
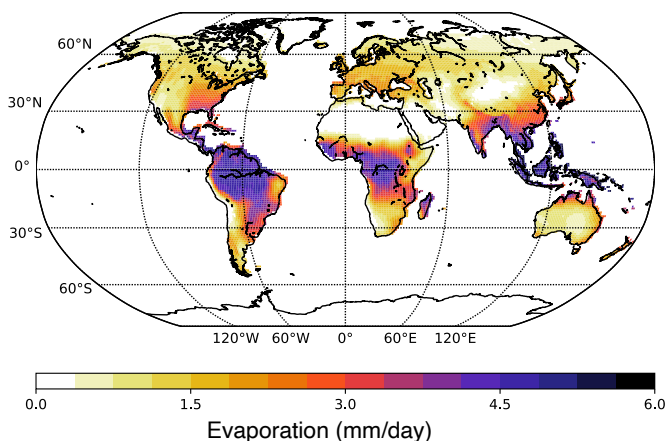
b. Comparison
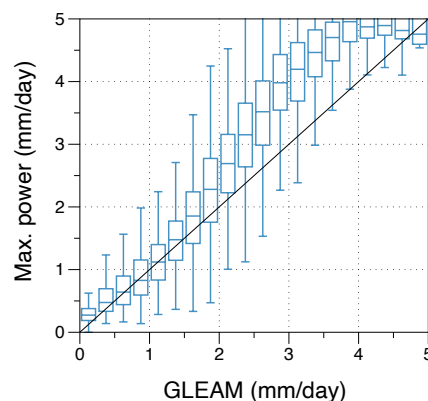
Figure 10. a. Annual mean evaporation derived from maximum power, thermodynamic equilibrium partitioning, and precipitation. b. Comparison of the estimate to the GLEAM evaporation dataset (Miralles et al., 2011; Martens et al., 2017). The linear regression among the two estimates yields a correlation coefficient of $r^2 = 0.85$ and a slope of $m = 1.25$. After Kleidon (2021b).

This partitioning represents two constraints of thermodynamics on evaporation: the maximum power limit sets the magnitude of buoyant exchange, and the thermodynamic equilibrium conditions at the surface set the magnitude of atmospheric

525   moistening by evaporation.

This thermodynamic estimate of evaporation can be evaluated using global radiation datasets (CERES, Loeb et al., 2018; Kato et al., 2018), combined with a precipitation dataset (GPCP, **?**) to account for the role of water limitation at the land surface, as in Kleidon (2021b). The climatological estimate derived in this way for the years 2003 - 2018 is shown in Figure 10 and is compared to the evaporation estimate of the GLEAM dataset (Miralles et al., 2011; Martens et al., 2017). Given that

530   this is a minimum approach to terrestrial evaporation, it reproduces the magnitude and continental variations in evaporation very well. This supports the interpretation made here of how thermodynamics and maximum power constrains the magnitude of hydrologic cycling.

This indirect application of thermodynamics to evaporation is consistent with boundary layer theory. Basically, the maximisation of power applies to the sensible heat flux, and this links directly to the buoyancy production term in the Turbulent

535   Kinetic Energy (TKE) budget of the boundary layer (see, e.g., textbooks by Stull, 1989; Arya, 1998). It can easily be shown that the buoyancy production term can be rewritten as a Carnot limit (Appendix C). Maximum power then corresponds to a maximisation of the buoyancy production term, which involves the interaction of the buoyancy flux with surface temperature, that is, that more buoyancy production results in stronger cooling of the surface. This effect is what leads to the maximum power limit, as shown in Section 2.4. Hence, thermodynamics adds an important and relevant constraint to surface-atmosphere

540   exchange as it limits the magnitude of the buoyancy production term in the TKE budget.

This maximisation of buoyancy production then shapes evaporation patterns on land, which is consistent with expressions for potential evaporation rates in hydrology, particularly the estimate by Priestley and Taylor (1972). While the Priestley-Taylor estimate includes an empirical coefficient of about 1.26, some studies have questioned the need for this coefficient when evaluating this estimate against observations at sub-daily scale (de Bruin et al., 2016; Conte et al., 2019). Hence, it
545 would appear that the concept of potential evaporation is equivalent with evaporation operating at its thermodynamic limit as described here.

This interpretation is, however, quite different to previous studies which applied MEP or related optimality approaches to evaporation (Wang et al., 2004, 2007; Wang and Bras, 2011; Kleidon and Schymanski, 2008; Porada et al., 2011; Yang and Roderick, 2019; Tu et al., 2022). Evaporation certainly produces entropy when saturated air is mixed with an unsaturated at-
550 mosphere near the surface. Yet, it requires transport for this mixing to take place, and this is accomplished mostly by buoyancy, even when the resulting sensible heat flux is often much smaller than the latent heat flux. While the outcome described here can be interpreted as an evaporation rate that is maximised given the constraints of the energy balance and mixing requirements (or its entropy production), it would obscure the central role of buoyant transport in shaping this outcome.

In summary, evaporation is an example for an Earth system process that reflects maximum power, but it is not directly
555 involved in the maximisation. Its magnitude is characterised by the thermodynamic equilibrium conditions at the surface where the phase transition takes place and by the buoyant transport, by which the vapour is transported and mixed into the atmosphere. As evaporation balances precipitation in the global mean, the strength of hydrologic cycling is thus strongly constrained by thermodynamics and optimality, although in a more indirect way. This interpretation is consistent with boundary layer theory, where maximum power adds a constraint to the magnitude of the buoyancy production term.

560 ### 3.3 Photosynthesis and terrestrial ecosystems

Photosynthesis, ecosystems, and life in general, represent an entirely different set of thermodynamic Earth system processes (Figure 11). They involve chemical transformations associated with their metabolic activities, which sustain their growth and maintenance of biomass, the dynamics of their populations and resulting food webs and, ultimately, biogeochemical cycles. Chemical reactions, in turn, involve changes in energy and entropy as chemical elements are arranged into different compounds.
565 Specifically, these changes apply to the energy by which electrons are bound to the nuclei and the random motion of molecules that we characterise as heat. These two forms of energy are associated with molar and thermal entropies. The second law of thermodynamics is reflected in these reactions aiming to minimise their Gibbs free energy, that is, free energy in chemical form (with the definition of free energy used here, this minimisation of Gibbs free energy is equivalent to a reduction of free energy to zero). To understand the factors that limit these dynamics relates to how much chemical free energy was generated in the
570 first place. This free energy is generated by photosynthesis. Hence, the question of how thermodynamics and optimality apply to ecosystems relates first and foremost to how it constrains photosynthetic activity within the Earth system. The generated free energy then sets the magnitude of the dissipative dynamics of the biosphere.

The efficiency of photosynthesis in generating energy in form of carbohydrates from sunlight has been evaluated over the last decades, theoretically (Duysens, 1958; Radmer and Kok, 1977; Landsberg and Tonge, 1980) and by using observations
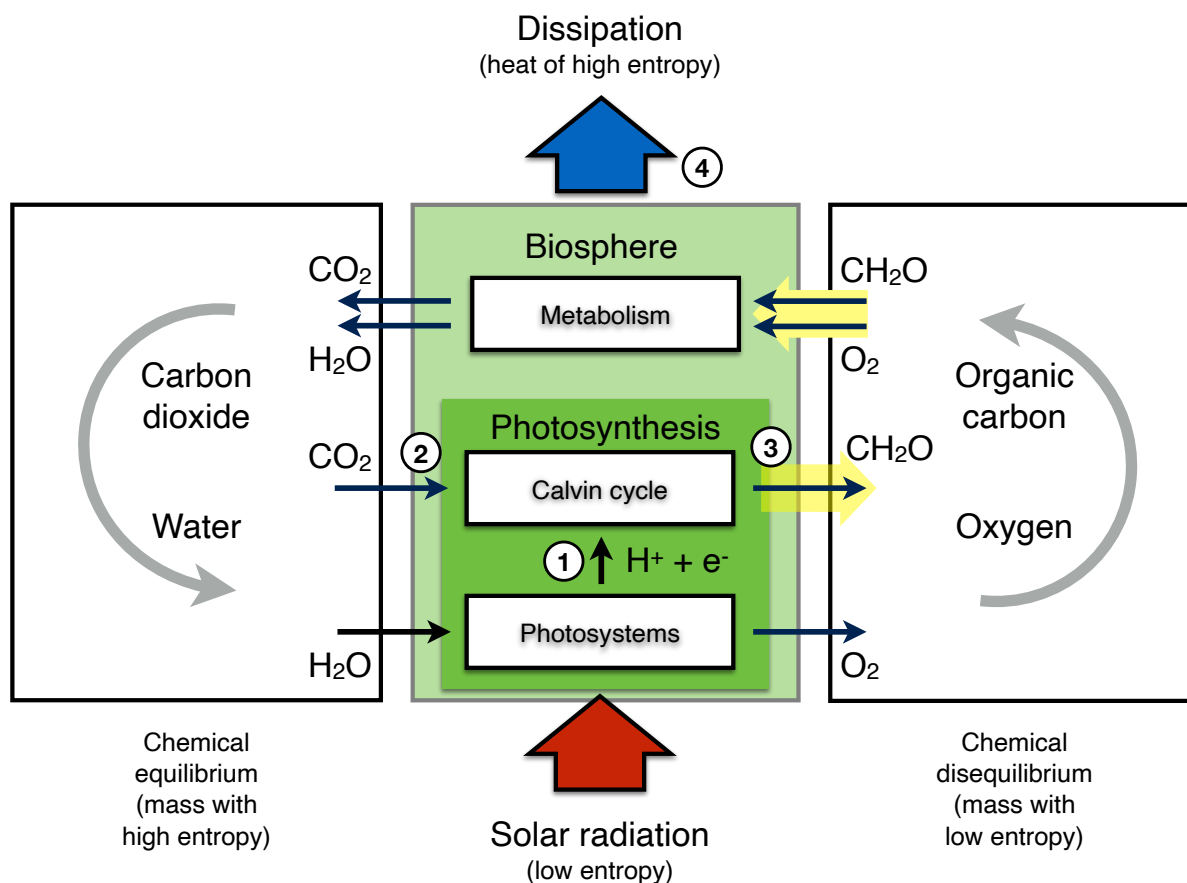
Figure 11. Thermodynamics of the biosphere, with solar radiation as the energy source of low entropy. The numbered circles mark places at which thermodynamic conversions and entropy production takes place: (1) Photosystems perform the work of charge separation in the light-dependent reactions; (2) CO_2 is taken up from the environment, requiring dissipative mixing as a transport mechanism; (3) The Calvin cycle converts CO_2 into carbohydrates in the dark reactions of photosynthesis using short-lived energy carriers; (4) The metabolic activities of the producers as well as of the consumers convert the chemical free energy in organic carbon back into heat, resulting in thermal entropy production. Overall, the activity of the biosphere is reflected in a state of chemical disequilibrium in form of reduced, organic carbon compounds and oxygen in contrast to carbon dioxide and water.

575 (Monteith, 1972, 1977). The first step in photosynthesis takes place in the photosystems, which use sunlight to split water and perform the work of charge separation (marked by circle (1) in Fig. 11). This converts the radiative energy of the solar photons with 680 and 700 nm wavelengths into electric energy in form of electrons and protons. This step is highly efficient. The photosystems require a minimum of eight photons for deriving the energy to fix one molecule of carbon dioxide (known as the quantum yield efficiency, e.g., Emerson (1958)). These photons yield 14.4 eV of energy, while it takes 13.6 eV to separate 580 the charges of the hydrogen atom. This first step in photosynthesis from radiation to electric energy thus seems highly efficient since most of the energy of the absorbed photons is transferred into electric energy.

The next steps incorporate this electric energy into ATP and further into sugars within the Calvin cycle (circles (2) and (3) in Fig. 11). The efficiency of the whole conversion from light to carbohydrates can then be estimated from the ratio of chemical energy output in form of carbohydrates to radiative energy input by absorbed light. Carbohydrates contain about 470 kJ/mol C of energy, while the photons supply an equivalent of about 1390 kJ/mol C (using the Avogadro number to convert the 14.4 eV to energy/mole). The ratio of energy output to input yields an efficiency of 470 kJ/1390 kJ = 34%, which is about what can be seen in the performance of photosynthesis in low light conditions (Hill and Rich, 1983). This would support the notion that photosynthesis operates near its theoretical limit. Observations of terrestrial ecosystems, however, show a much lower efficiency with less than 3% of the absorbed solar radiation being converted by carbon uptake (Monteith, 1972, 1977). Does this much lower efficiency observed in ecosystems imply that their activity is not constrained by thermodynamics?

This apparent discrepancy in efficiency can be explained by considering that it is the gas exchange of carbon dioxide and water between the vegetative cover and the atmosphere that limits carbon uptake by terrestrial ecosystems, and that this gas exchange is limited by thermodynamics (Kleidon, 2021b). To bind the solar energy into carbohydrates, vegetation needs to take up carbon dioxide from the atmosphere, and in doing so, inevitably loses water. This gas exchange is well known. It takes place through the stomata of the leaves, and results in the evaporation rate over vegetated land being dominated by the transpiration of vegetation. Evaporation in itself is a strongly thermodynamically controlled process, as just described in Section 3.2, and consequently, the gas exchange of water vapour is as well. The ratio of the simultaneous exchanges of water vapour and carbon dioxide, the so-called water use efficiency, is relatively fixed across ecosystems, with values between 2 - 4 grams of carbon uptake for a kilogram of water lost, as inferred from flux measurements (Law et al., 2002) or derived from global datasets (Kleidon, 2021b).

When we combine the water use efficiency with the factors that set the thermodynamic limit of evaporation, we obtain an estimate for the efficiency by which photosynthesis converts sunlight into carbohydrates. This efficiency is the combination of diverse losses: To start, about 50% of the absorbed solar radiation is partitioned into turbulent heat fluxes at maximum power (Section 2.4) while the other half is lost by the exchange of thermal radiation. Then, 70% of the turbulent heat fluxes are represented by the latent heat flux (using Eq. 15 for global mean conditions), resulting in the evaporation rate when the supply of water does not limit evaporation. When the vegetative cover transpires one kilogram of water vapour, this contains about 2.5 MJ of latent heat. Using the median water use efficiency from observations of 2 gC/kgH2O (Kleidon, 2021b), two grams of carbon are being taken up, able to incorporate 78 kJ of chemical energy (2 gC x 470 kJ/12 gC). This yields an overall efficiency of 50% (maximum power partitioning) x 70% (partitioning into latent heat) x 78 kJ/2.5 MJ (water use efficiency) = 1%. This value reproduces the low efficiency reported for terrestrial ecosystems. A more detailed evaluation of the resulting pattern of the efficiency of photosynthetic carbon uptake (Figure 12) resembles closely the pattern inferred from a more complex terrestrial carbon cycle model (Randerson et al., 2017; Ott, 2020). This implies that the photosynthetic activity of terrestrial ecosystems is indeed thermodynamically constrained, but not directly by the conversion of light into carbohydrates, but rather by solar radiation being the driving force for the gas exchange needed to supply plants with carbon dioxide.

This interpretation of how thermodynamics limits the activity of terrestrial ecosystems is consistent with established notions in plant ecophysiology, such as the central role of water use efficiency in ecosystem productivity and their response to

a. Carbon uptake efficiency estimate
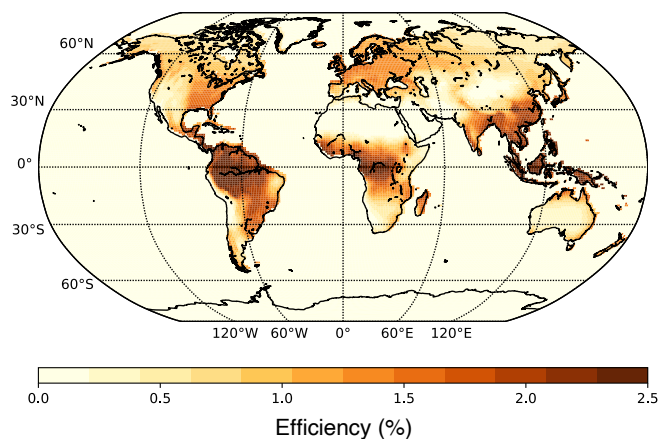
b. Comparison
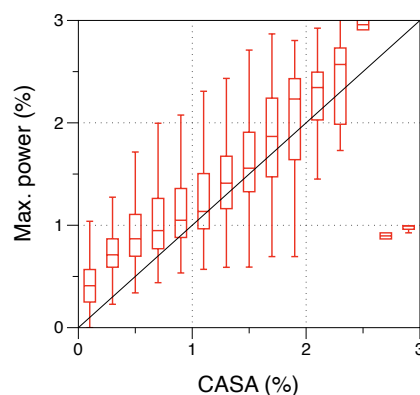
Figure 12. a. Thermodynamic efficiency of terrestrial carbon uptake by photosynthesis estimated using the thermodynamically constrained gas exchange based on maximum power. (b.) Comparison of the thermodynamic efficiency to an estimate derived from the CASA biosphere model (Randerson et al., 2017; Ott, 2020). The linear regression among the two estimates yields a correlation coefficient of $r^2 = 0.56$ and a slope of $m = 0.79$. After Kleidon (2021b).

atmospheric concentrations of carbon dioxide (e.g., Schimel et al., 2015). It provides novel insights, because it identifies a different, relevant limitation on ecosystem productivity. Typically, ecosystem productivity is viewed as being either light- or water limited (Churkina and Running, 1998), and these limitations are formulated in semiempirical ways. When looked at it 620 from thermodynamics, it shows that light is not a limiting factor, but rather the gas exchange, which in turn is driven by solar radiative heating. In other words, the correlation in observations between light availability and productivity at the ecosystem scale does not originate from light limitation, but rather from a transport limitation, which in turn is driven by absorption of sunlight. This supports the well-established notion that the large-scale patterns of terrestrial productivity are shaped by climate. What this interpretation adds is that these patterns reflect the operation of photosynthetic carbon uptake at the limit indirectly 625 set by thermodynamics.

This interpretation is, however, quite different to previous applications. Previous studies applied maximum power to ecosystems in a quite general way without being explicit of how this relates to the environment (Lotka, 1922a, b; Odum and Pinkerton, 1955). Other studies interpreted the greater absorption of solar radiation by vegetated surfaces compared to bare ground as a direct manifestation of ecosystems maximizing their entropy production (e.g., Ulanowicz and Hannon, 1987; Schneider and 630 Kay, 1994; Holdaway et al., 2010; Schymanski et al., 2010; del Jesus et al., 2012). Here, again, the interpretation described above does not contradict these more qualitative interpretations, but offers a more differentiated picture. Life does not simply enhance entropy production. It requires gas exchange to produce carbohydrates, and as this is driven by absorption of solar radiation, a lower surface albedo can drive more buoyancy and be advantageous in that it reduces the limitation imposed by gas exchange. So there is a beneficial effect for photosynthetic carbon uptake, which allows for more biospheric activity. It

635 also enhances the entropy production by absorption of solar radiation, but this in itself has no benefit for biospheric activity. This more differentiated interpretation thus links thermodynamics and optimality of life closer to the actual processes that are needed to sustain the dissipative activity of the biosphere.

There are other biotic effects that can enhance carbon uptake further and thus the power generated. Deep roots allow for greater seasonal water storage within the soil, allowing vegetation to enhance its productivity and evaporation during dry peri-

640 ods (Nepstad et al., 1994; Kleidon and Heimann, 1998; Miguez-Macho and Fan, 2012; Wang-Erlandsson et al., 2016). From a thermodynamic perspective, this corresponds to maximising the period of gas exchange and thus photosynthetic activity when evaporation is thermodynamically constrained rather than constrained by water accessibility. Optimising stomatal conductance can enhance carbon uptake for given water loss, resulting in behaviour that is consistent with theory and empirical relationships (Cowan and Farquhar, 1977; Katul et al., 2009; Medlyn et al., 2011). This would maximise carbon uptake and photosynthetic

645 activity for a given water loss set by thermodynamic or water availability constraints. These effects can then result in rainforest evaporation during dry periods at rates solely set by thermodynamics (Conte et al., 2019). This does not contradict the notions that ecosystems maximise, alter their environment, or that they are dominated by thermodynamic constraints. It rather implies that when they do maximise their power associated with carbon uptake, they reach the limit imposed indirectly by thermodynamics, thus making the process predictable by thermodynamics and optimality.

650 To sum up, carbon uptake by terrestrial vegetation is another example of an Earth system process that appears to reflect maximum power, but in an indirect way, similar to how evaporation is indirectly constrained by maximum power. The bottleneck appears to be the gas exchange between the vegetated surface and the lower atmosphere. It is reflected in the observed, relatively uniform value of water use efficiency across terrestrial ecosystems. This interpretation is consistent with the common recognition of the importance of water use efficiency for terrestrial ecosystems, it can explain the low efficiency of photo-

655 synthetic carbon uptake. It provides a novel perspective of how integrated vegetation productivity is with land-atmosphere exchange, and how thermodynamics and optimality apply to ecosystem activity.

3.4 Putting things together

To quickly summarise these examples, let us place them back into the thermodynamic view of the Earth system shown in Figure 1. Generating vertical and large-scale horizontal motion, as described in Sections 2.4 and 3.1, deals with heat engines

660 that convert differences in radiative heating into the free kinetic energy associated with motion (shown at the top of Figure 1). The heat transported by motion reduces the temperature difference (shown by the dashed line on the right of Figure 1), and this interaction results in the maximum power limit of these heat engines. The fluxes and temperatures that result from this thermodynamic maximization compare very well with observations at the climatological scale, providing support that thermodynamics and optimality play a dominant role in planetary functioning.

665 The other two examples, terrestrial evaporation (Section 3.2) and carbon uptake by vegetation (Section 3.3), are shaped by this thermodynamic limit associated with motion (the next two inner shells shown in Figure 1, entitled "Cycling" and "Life"). For evaporation, it is the combination of the partitioning of absorbed radiation into heating and moistening of near-surface air with the maximum power limit of generating vertical convective motion that sets the dominant constraint. For carbon uptake

of vegetation, the energy supply is not heat, but the direct use of sunlight (as shown by the yellow box "Photosynthesis" in
670 Figure 1). Yet, the magnitude is limited by the gas exchange of carbon dioxide associated with buoyant mixing between the
canopy and the lower atmosphere. This constraint set by gas exchange can explain the low observed thermodynamic efficiency
of photosynthesis of natural ecosystems. These two examples thus demonstrate that their magnitudes are constrained indirectly
by thermodynamic limits, but not by the heat flux - temperature difference trade-off that is at the center of the maximum power
limit for generating motion. This emphasises the importance of looking at the relevant details of the processes involved in
675 limiting planetary processes and their connections to transport as they do not fit into a generalised maximisation template as
suggested, for instance, by the proposed MEP hypothesis.

4   Thermodynamics, optimality and Earth system science: Synthesis and what's next?

The examples provided in the last section support the overarching view of how thermodynamics and optimality limit the
Earth system and shape its functioning. In the following, I first discuss some of the limitations and potential extensions of the
680 approach, link previously suggested optimality approaches to the view described here, and describe a few of its applications to
do simple, physics-based Earth system science.

4.1   Limitations and potential future extensions

There are, of course, several potential limitations of the formulations described here. After all, these formulations are kept as
simple as possible, so there is ample space of further improvement and refinement. In the following, I want to briefly describe
685 some of these limitations and how they could affect the application of thermodynamic limits.

In the applications of maximum power to atmospheric heat engines and associated motion, using radiative temperatures as
the cold temperature for the heat engines is optimistic as it assumes that the emitted radiation to space is emitted at maximum
entropy. Outgoing longwave radiation, however, is emitted as a mix from different levels of the lower atmosphere, so its entropy
is below its maximum value. This would then affect the outcome of the optimisation, resulting in less power and the values of
690 the fluxes shifted to lower values (as, for instance, shown by Dhara et al., 2016). In the example of large-scale atmospheric heat
transport, the conservation of angular momentum was not considered, so that the outcome of maximum power is independent
of the Earth's rotation rate. This outcome has been criticised by Goody (2007) in the context of the MEP hypothesis. There
are a few attempts to include this constraint in the maximisation (Jupp and Cox, 2010), with the result then depending on
the rotation rate, less power is generated, and less heat being transported. Also, the diurnal cycle and seasonality result in
695 heat storage changes within the atmosphere that affects the Carnot limit, because these are associated with entropy changes
within the system. This affects the outcome of the maximisation, the resulting power and fluxes (Kleidon and Renner, 2018).
While these points would certainly affect the outcome of thermodynamic optimality, they are unlikely to substantially alter
the conclusion that these engines operate near their limit, because the agreement with observations is already rather good. The
refinements described here are likely to improve the comparison to observations.

700   Evaporation was then related to maximum power indirectly by the transport limitation associated with generating vertical convective motion from the local radiative forcing. What this excludes is the contribution by moist convection, that is, the generation of vertical motion due to condensational heating within the atmosphere, and the contribution by mixing by surface friction from the large-scale circulation. These effects could play a role at certain times and in certain regions, for instance open water surfaces, where heating is much weaker than over land. Yet, the agreement with observation-based datasets is

705 already very good, which suggests that these contributions are comparatively minor, at least on land, so that evaporation is predominantly shaped by the thermodynamic limit based on the local radiative forcing. This has some interesting implications that can be explored in future research, such as the lack of a dependency on the water vapor pressure deficit (which is, for instance, assumed in the Penman-Monteith equation, Monteith (1965)). It may further help to improve the semi-empirical stability functions in drag parameterizations in climate models, where surface-atmosphere exchange is predominantly shaped

710 by the frictional dissipation of large-scale wind fields.

    Carbon uptake by vegetation was associated with the generation of vertical convective motion, so that the thermodynamic constraint applies indirectly, as in the case of evaporation over land. What this interpretation did not explain yet is the value of the water use efficiency that was derived from observations. In principle, it should be possible to derive this value from this approach as well, but it would require a refined representation of surface-atmosphere exchange. Specifically, it would need to

715 represent the temperature difference between the surface and the near-surface atmosphere as it is this temperature difference that relates to buoyancy production at the surface as well as the exchanges of water vapor and carbon dioxide. This would require further research, it could be compared to the wealth of data available from eddy covariance measurements, and could provide a simple, physics-based understanding of how this important property would potentially change under different climates. This would, however, not change the conclusion that thermodynamics and optimality apply mostly indirectly to vegetation activity

720 through constraining gas exchange.

    Overall, the conclusion that thermodynamics and optimality apply predominantly in form of the maximum power limit from radiative heating to generating motion, and that the resulting motion then predominantly shapes associated Earth system processes would remain unaffected.

4.2   Optimality in context of the thermodynamic Earth system

725 I next want to relate this view of thermodynamics and optimality to other, previously suggested thermodynamic optimality approaches. A diverse range of thermodynamic optimality approaches have been suggested, focusing mainly on either minimizing or maximizing entropy production, power or dissipation. At first, it would seem that these contradict each other. What I want to show in the following is that it is mostly a matter of perspective, and that the focus on work being done and on the whole system helps to differentiate between these.

730   We start by taking a look at the thermodynamic setting of the whole Earth system, which is characterized by the planetary entropy budget. This budget is almost entirely determined by how much solar radiation is being absorbed. If we exclude potential effects of albedo changes due to clouds and ice, this fixes the rate of absorption of solar radiation. This, in turn, fixes the magnitude of energy conversions as well as the total radiative entropy exchange by setting the radiative temperature
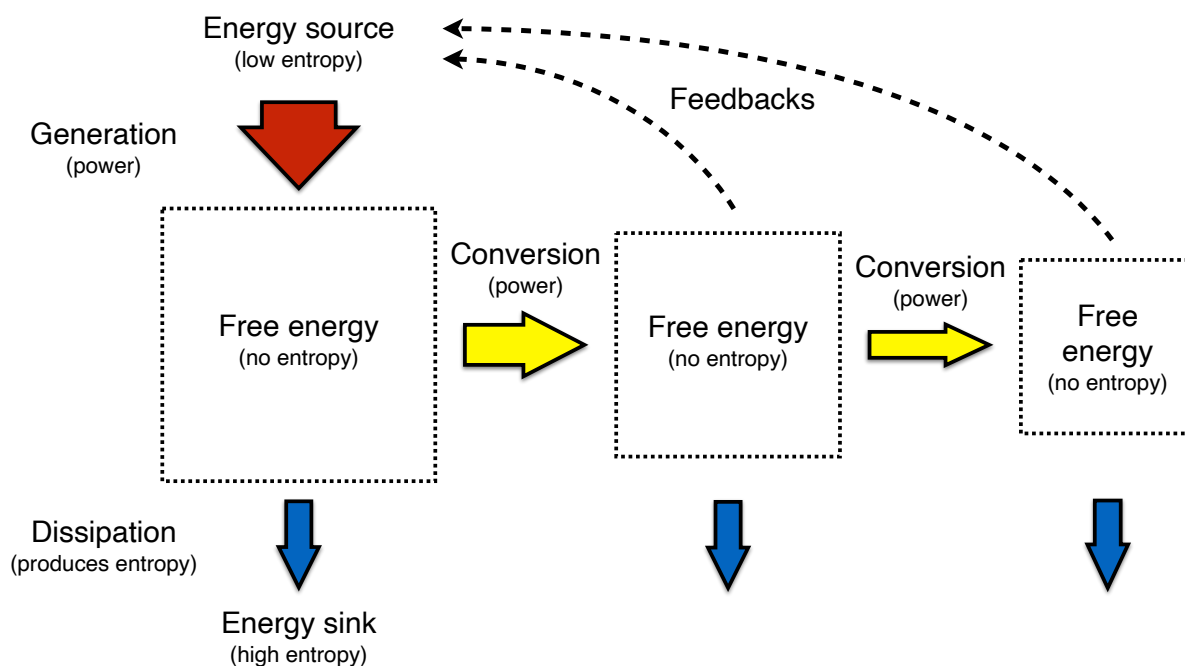
Figure 13. Once free energy is generated from an energy source of low entropy, it can either be converted into another form of free energy by performing work or dissipated back into heat of high entropy. This can form a sequence of free energy conversions. Maximum power can also apply to these further conversions, or to the feedbacks that these processes have on the forcing of the generation process. See text for examples of Earth system processes.

of the emitted radiation to space. This leads to an almost fixed entropy exchange of the planet, so that the overall entropy
735   production by Earth system processes is fixed as well (which can also be seen in Fig. 8b). What this implies is that when one
process enhances its entropy production, this comes mostly at the cost of another. In relation to optimization, it implies that
when one process maximizes entropy production, the entropy production of other processes is minimized. It is thus a matter of
perspective of which process is being looked at whether something is minimized or maximized, even if it sounds contradictory
at first.
740   We next need to distinguish between processes that simply dissipate and produce entropy from those that perform work,
generate free energy, drive the dynamics of dissipative structures and produce entropy when this free energy is dissipated (as
described in Section 2.2, and shown in Figure 1 by the yellow boxes). When atmospheric processes operate at maximum power,
they also maximize dissipation and associated entropy production. This maximization comes at the expense of reducing, or
even minimizing, the entropy production by radiative exchange, which does not involve work being done, no free energy is
745   generated and dissipated. The focus on work and the resulting generation of free energy is thus a critical aspect to distinguish
Earth system processes, and it is those processes to which maximum power potentially applies to.

The application of optimality, however, does not only apply to the conversion of low-entropy solar radiation into free energy. Once free energy is generated from the solar forcing, it can either be directly dissipated, or converted into another form of free energy before it is eventually dissipated (Figure 13). This can result in sequences of free energy conversions. To these

750 sequences, maximum power may also apply by maximizing the rate of free energy transfer down the sequence. An example for such a conversion chain in the climate system is the conversion of a fraction of the kinetic energy of atmospheric motion into wave energy at the ocean surface, with the other part of the free energy lost by frictional dissipation within the near-surface atmosphere. Wave energy is converted further into the kinetic energy of the wind-driven ocean circulation, with dissipative losses during the conversion. Maximum power in this context does not involve entropy, as it involves the maximized conversion

755 of free energy into another form. Two examples in the literature of such applications of maximum power are the shaping of dunes by winds (Rubin and Hunter, 1987) and the physical limits of using wind energy as renewable energy at large scales (Miller et al., 2011; Miller and Kleidon, 2016; Kleidon, 2021a). It may also apply to the feedbacks that these sequences have on the forcing that would enable a higher generation rate (shown by the dashed lines in Figure 13), for instance by altering the radiative forcing. It remains to be seen how general the application of maximum power in such free energy conversion

760 sequences is, leaving ample opportunities for future research.

We can also apply this view of free energy conversion sequences to hydrology. A line of research applied "minimum energy expenditure" to understand fractal river networks (Rinaldo et al., 1992; Rodriguez-Iturbe and Rinaldo, 1997). This energy expenditure essentially relates to the minimisation of frictional dissipation within channel networks, similar to how frictional dissipation is minimised in vascular networks (West et al., 1999). This minimisation fits into the picture here when we look at

765 the whole system (Kleidon et al., 2013), and aim to understand the response of the whole catchment (Savenije and Hrachowitz, 2017). Rainfall at a certain elevation above sea level represents an input of free energy in form of potential energy, energy that was generated by hydrologic cycling by a moist heat engine driven by condensational heating within the atmosphere. The input of free potential energy is converted into kinetic energy as water flows downhill, which is dissipated due to friction with the Earth's surface. When fractal river networks then minimise the frictional losses of water flow by the transition from sheet flow

770 to channel flow (reducing the wetted perimeter per transported volume), it implies that the kinetic energy of the water flow performs maximum work on maintaining the flow and sustaining sediment transport. It represents one step in a free energy conversion sequence, starting with an atmospheric heat engine performing the work to lift water, and minimisation of frictional dissipation being synonymous with the maximum power transfer to sediment transport along this conversion sequence.

Ecosystems also represent such free energy conversion sequences that are fuelled by photosynthesis (rather than heat en-

775 gines). Maximum power has been suggested to apply to living organisms dating back to Lotka (1922a; 1922b), with extensions to ecosystem development (Odum and Pinkerton, 1955; Odum, 1988; Fath et al., 2001; Joergensen, 2001; Hall, 2004). In principle, these previous applications are consistent with the view described here. There is nevertheless somewhat of a difference in terms of the focus. Here, the focus is not on the ecosystem itself, that is, the conversion sequence after the free energy was generated from the solar forcing, but rather on the link with the Earth's physical environment in which the free energy

780 is being generated and how it acts to constrain this generation. This results in an interesting mismatch: While the constraint on biospheric activity derived here results in a flux per unit surface area, ecosystems operate with individual organisms. The

missing link to overcome this apparent mismatch is accomplished by self-thinning laws, relationships that describe how the number of organisms within a certain area changes with their respective size. In this context, Enquist et al. (1998) have provided a simple, physical explanation for such self-thinning laws in tree communities given a resource constraint expressed per

785   unit area (the total flux of water through xylems of the trees, which characterizes transpiration rate and carbon uptake). This work would directly connect the constraint described here to the organism-based view of ecosystems. Subsequent conversions of energy in food chains would then represent energy conversion sequences shown in Figure 13. The maximum power limit could potentially apply to each conversion step from one trophic level to the next, and it would include potential feedbacks by the effect of higher trophic levels on the producers, for instance by enhanced nutrient cycling (e.g., McNaughton, 1979; Vanni,

790   2002; Wolf et al., 2013; Buendia et al., 2018) that would allow for higher productivity or by changing the radiative forcing for the heat engines by changing greenhouse gas concentrations at geological time scales (Schwartzman and Volk, 1989; Berner, 1997; Kasting and Catling, 2003).

To conclude this discussion on thermodynamics and optimality within the Earth system, these examples show that there is ample room for further applications of maximum power and optimality to different aspects of Earth systems. Most of these

795   applications would not involve thermodynamics directly, because maximum power would apply to the further conversion of free energy along energy conversion sequences. What I have described in the examples above, and is depicted in Figure 1, is merely the first step for a full description of these energy conversion sequences and their effects on the Earth system. This first step focuses on the processes that generate free energy from the solar forcing and represent the beginning of free energy conversion sequences (yellow boxes in Figure 1 and the leftmost box in Figure 13). This first step shows us that the overall, dissipative

800   dynamics of Earth system processes are constrained and characterized very well by the combination of thermodynamics and optimality at a rather simple, yet profound physical level.

4.3   Applications to Earth system science

At the end, I want to briefly describe three examples of how this thermodynamic Earth system approach can inform Earth system science.

805   The first example is the controversial Gaia hypothesis of Lovelock (1972a, b), which states that the Earth system with life is a self-regulatory system exhibiting homeostatic behavior at the global scale. While this may seem far-fetched, Lovelock's motivation came from the thermodynamics of life of Lotka (1925) and Schrödinger (1944), and the recognition that the Earth's chemical disequilibrium within the atmosphere is an imprint of life (Lovelock, 1965). In the context of the thermodynamic Earth system view described here, such homeostatic outcome can be imagined as the consequence of a biosphere that operates

810   at its maximum power limit and the resulting interactions with the physical environment (Kleidon, in press). Section 3.3 showed that it is the physical gas exchange that limits biotic productivity, so that maximum productivity is intimately linked to a maximum in the gas exchange rate. At larger spatial and temporal scales, biotic productivity removes carbon dioxide from the atmosphere, which alters its greenhouse effect. The greenhouse effect, in turn, alters the radiative environment, which in turn can affect the outcome of the maximum power limit, and thereby the intensity of gas exchange. This could, in principle, result in

815   an optimum state of the greenhouse forcing that would allow for maximum productivity. Such maximisation would then result

in self-regulating behaviour, just like how atmospheric convection apparently self-regulates to maximise its power. As carbon dioxide is transformed by photosynthesis into reduced carbohydrates (in form of biomass) and atmospheric oxygen, this state would also reflect chemical disequilibrium of the Earth system. The outcome would then be rather similar to the postulated behaviour of the Gaia hypothesis, yet result as an outcome of thermodynamic maximisation associated with the biosphere and
820   the interactions with the abiotic environment (Kleidon, in press). This would, however, require further evaluations.

The second example deals with more practical and quantitative applications to the Earth system response to global climate change. The maximum power limit has been applied to back-of-the-envelope estimates of how the hydrologic cycle responds to global warming and solar geoengineering (Kleidon and Renner, 2013b), its transient response (Kleidon et al., 2015a), and to explain the land-ocean contrast in climate sensitivity (Kleidon and Renner, 2017). In each example, maximum power serves as a
825   constraint to close the surface energy balance (as in Sections 2.4), so that analytical expressions were derived for the responses. The outcomes closely resemble the simulated responses of global climate models, demonstrating that thermodynamics and optimality dominate the response of the climate system to change. This should help us to advance our physical understanding of the dominant effects of global climate change that does not depend on the highly complex and often incomprehensible numerical simulation models. There are certainly many other aspects of global climate change that could be evaluated from
830   this approach.

The last example is perhaps the most relevant in terms of practical implications. By focusing on how much work different processes in the Earth system can at best perform, this yields estimates of different forms of free energy that could in principle be used as renewable energy (Figure 14). The different means to generate free energy are shown in Figure 1 by the three yellow boxes, and they vastly differ in their efficiencies. Atmospheric heat engines can only convert about 10% (vertical)
835   or 1% (horizontal) of the total absorbed solar radiation into kinetic energy and other forms derived from it. Photosynthesis operates with a somewhat similar efficiency of 1-2% of turning solar radiation into chemical energy in form of biomass. Yet, photovoltaics has a theoretical efficiency above 70% (Press, 1976; Landsberg and Tonge, 1979). This much higher efficiency is possible because it does not use heat (like an atmospheric heat engine), and it is not constrained by gas exchange (like photosynthesis). Hence, photovoltaics has a much greater potential to yield renewable energy than all other forms of renewable
840   energy combined. This important insight comes directly from the application of thermodynamic limits in combination with an Earth system view, as the latter can explain why other forms of generating free energy are much less efficient than photovoltaics.

These three examples illustrate that the combination of thermodynamics, limits, and interactions can provide a range of different insights for Earth system science. Clearly, there is ample space for future work. It does not mean to "reinvent the wheel", but rather a change in perspective. This perspective should focus on the work done and the free energy being generated
845   by Earth system processes, where this free energy comes from, what it does, which factors constrain its generation, and what the consequences are. This should allow us to gain a more robust physical understanding of Earth system processes as well as the role of interactions. It would allow us to understand the emergent simplicity of patterns and functioning in the Earth system by attributing this simplicity not to the simplicity of the processes involved, but rather to the notion that the dynamics are so complex and well tuned that these operate at the thermodynamic limit. This understanding should then further allow us to
850   evaluate how Earth system processes evolve and react to change, not in terms of the usual state variables such as temperature,
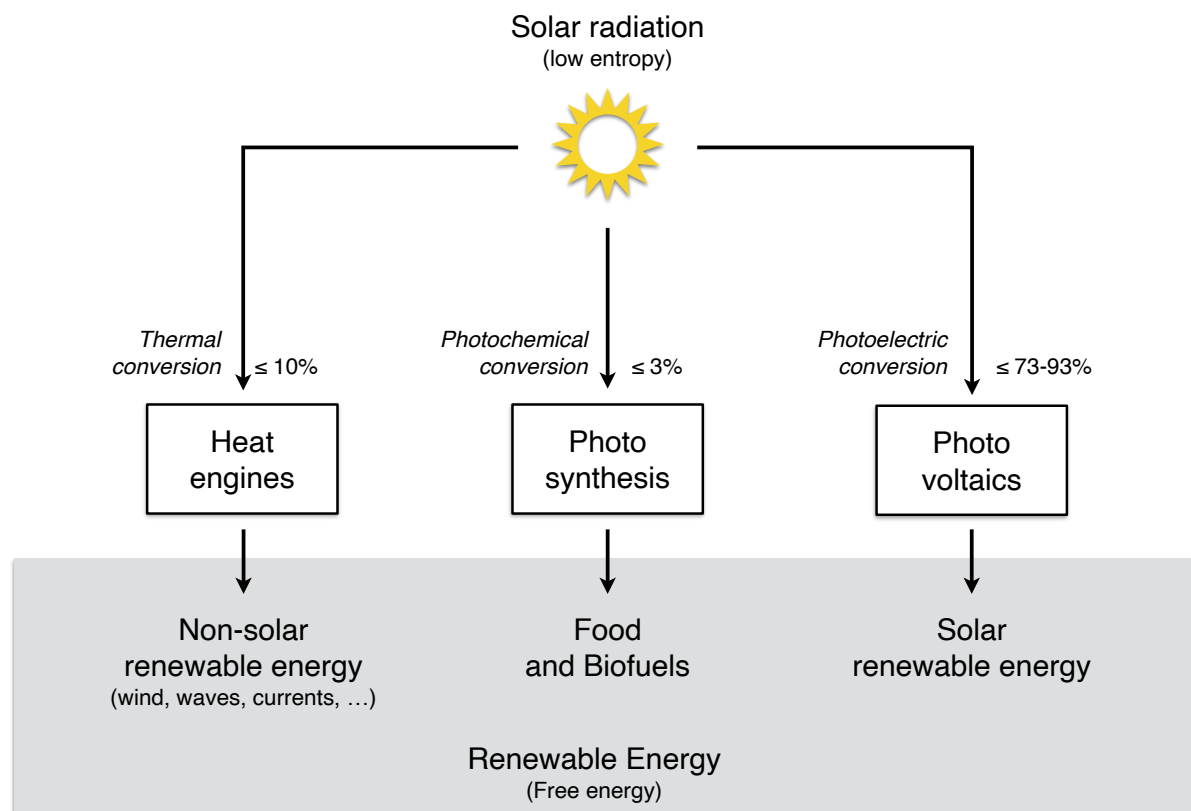
Figure 14. Ability to generate free energy from solar radiation at the planetary scale that could be used as renewable energy and their associated efficiencies (after Kleidon et al. (2015b)).

but rather in terms of how the ability to perform work is affected and how the dissipative behaviour of the associated processes is going to change. In the end, this would imply that essentially all Earth system processes, from the physical processes of the climate system to the various activities in human societies, can be described by the same formalisms and concepts, allowing us to identify limits and generalities across the functioning of various Earth systems.

5 Conclusions

This review dealt with thermodynamic optimality approaches, aiming to provide a general and unifying view of how these apply to and shape Earth system functioning. At the core is the second law of thermodynamics. While every process needs to obey this law, I showed that the relevant constraint comes from its role in limiting how much work can be derived from the solar radiative forcing, generating free energy of some form. The relevance of thermodynamics to Earth system functioning thus boils down to its role in shaping the conversion of sunlight into work.

There are basically three different processes that accomplish this work in the Earth system: (i) heat engines convert differential heating and cooling into work, generating motion and shaping the emergent characteristics of the climate system; (ii) photosynthesis converts solar radiation directly into chemical free energy without heat being involved, shaping the dynamics of the biosphere; and (iii) photovoltaics converts solar radiation directly into electricity, which has the potential to shape human societies in the future. The derived work generates free energy, and the dynamics within the associated systems convert this free energy in sequences into other forms before turning it back into heat with high entropy.

Thermodynamics and optimality then constrains the intensity of these energy conversion sequences by limiting the conversion of sunlight into work. For heat engines, optimality applies in terms of the maximum power limit. This limit originates from the combination of the well-established Carnot limit with the important effect of heat transport associated with motion, as this depletes the thermodynamic driver for deriving work, that is, it diminishes the efficiency term in the Carnot limit. This effect results in the maximum power limit. The examples in Section 3 showed that this maximum power limit can very well predict the magnitude of heat transport in the climate system as well as the distribution of surface temperatures. It then indirectly sets the magnitudes of hydrologic cycling and carbon exchange of terrestrial vegetation, because these two processes are limited by the transport that the heat engines of the climate system generate. We can thus understand the emergence of simple, climatological patterns as the reflection of atmospheric heat engines working as hard as they can, with its implications manifesting itself in the linkages to other processes and further down the energy conversion sequences.

In conclusion, I hope that this thermodynamic Earth system view provides a more differentiated view of the critical role that thermodynamics and optimality play in shaping the Earth system. Different, seemingly contradictory approaches such as minimizing dissipation or maximizing power are not in contradiction, but a matter of how processes fit into the sequences of energy conversions once free energy is generated. This should provide ample opportunity for future research and understanding. After all, it would seem indisputable that performing work is of central importance for driving dynamics. It thus seems surprising that this focus on work and the factors that limit it has so far essentially been absent in Earth system science.

Appendix A: Entropy budget estimation

The thermal entropy budget terms shown in Figure 8b and d are estimated as follows.

The entropy production by absorption of solar radiation within the two boxes, $\sigma_{s,t}$ and $\sigma_{s,p}$, is estimated in terms of the thermal entropy production (i.e., neglecting the expansion of the photon gas, which results in the factor of 4/3 in expressions for radiative entropy production, e.g., Lineweaver and Egan (2008))

$$\sigma_{s,t} = R_{s,t} \left(\frac{1}{T_{sun}} - \frac{1}{T_{s,t}} \right) \tag{A1}$$

and

$$\sigma_{s,p} = R_{s,p} \left(\frac{1}{T_{sun}} - \frac{1}{T_{s,p}} \right) \tag{A2}$$

with $T_{sun} = 5760$ K being the emission temperature of the Sun.

The entropy production by longwave exchange as well as convective motion within each of the two boxes are estimated using the respective surface and radiative temperatures

$$\sigma_{l,t} = R_l(T_{s,t}) \left(\frac{1}{T_{r,t}} - \frac{1}{T_{s,t}} \right) \tag{A3}$$

895   and

$$\sigma_{l,p} = R_l(T_{s,p}) \left(\frac{1}{T_{r,p}} - \frac{1}{T_{s,p}} \right) \tag{A4}$$

where $R_l(T)$ is given by Eq. 10.

Entropy production by frictional dissipation, σ_{fric}, is estimated from the generated power by

$$\sigma_{fric} = \frac{1}{2} \cdot J \cdot \left(\frac{1}{T_{s,p}} - \frac{1}{T_{s,t}} \right) = \frac{1}{2} \cdot J \cdot \left(\frac{T_{s,t} - T_{s,p}}{T_{s,p} T_{s,t}} \right) \tag{A5}$$

900   where the factor of 1/2 is included to account for heat being transported from one hemisphere to another. Note that this expression is equivalent to the generation of kinetic energy at the Carnot limit and its subsequent dissipation at $T_{s,p}$. This expression is also equivalent to the thermal entropy production of mixing heat with temperature $T_{s,t}$ in the colder reservoir $T_{s,p}$ at a rate J.

The total thermal entropy production, σ_{total}, is then given by the sum of these contributions

905    $$\sigma_{total} = \frac{1}{2} \left(\sigma_{s,t} + \sigma_{s,p} + \sigma_{l,t} + \sigma_{l,p} \right) + \sigma_{fric} \tag{A6}$$

The factor of 1/2 is included here again for averaging.

Appendix B: Estimating available potential energy

We can infer the available potential energy associated with the maximum power limit and compare it to estimates of the Lorenz Energy Cycle (LEC) from observations. To do so, we consider the vertical stratification in the atmosphere to be in hydrostatic
910   equilibrium, an assumption similar to those made in estimates of the LEC terms. This equilibrium is modulated by air density, with a warmer atmospheric column having a lower density, less pressure drop with height, and hence a greater potential energy. This potential energy U_{pe} can then simply be estimated by

$$U_{pe} = \frac{p_s}{g} \cdot R_a \cdot T \tag{B1}$$

with p_s/g being the overall mass of the atmosphere per unit area with p_s being surface air pressure, g the gravitational
915   acceleration, and R_a the gas constant for air.

The temperature difference described by the two-box model (cf. Eq. 11) thus also describes a difference in potential energy,
$\Delta U_{pe} = U_{pe}(T_{s,t}) - U_{pe}(T_{s,p})$. This difference, compared to the global mean, is shown in Figure 8f. With no heat transport,
the temperature difference is largest, and so is the difference in ΔU_{pe}. With increasing heat transport and a lower temperature
difference, this difference in ΔU_{pe} declines as well.

920   However, only a fraction represented at best by the Carnot efficiency is available for conversion of ΔU_{pe} into available
potential energy, A, equivalent to the conversion of the heat flux into kinetic energy. We thus get for A the expression (Kleidon,
2021a):

$$A = \frac{1}{2} \cdot \left(\frac{R_a p_s}{g} \right) \cdot (T_{s,t} - T_{s,p}) \cdot \frac{T_{s,t} - T_{s,p}}{T_{s,t}} \tag{B2}$$

Appendix C: Power and buoyancy production

925   A correspondence of maximum power associated with the sensible heat flux with maximum buoyancy production can directly
be obtained when considering the buoyancy flux. This flux is commonly written as $\rho w' \theta'$, with ρ being the air density (which
is often left out in the notation for the Turbulent Kinetic Energy (TKE) budget, e.g., in the textbook of Stull (1989)), w' the
variation in the vertical wind component and θ' the variation in potential temperature. The buoyancy production term in the
TKE budget, G_b, is then

930   $$G_b = \frac{g}{\theta} \cdot \rho w' \theta' \tag{C1}$$

where g is the gravitational acceleration and θ is the mean potential temperature of the boundary layer.

This buoyancy production term can be linked to maximum power by first integrating it over the height of the boundary
layer, z_b, to get the total buoyancy production in units of W m^{-2} to make it comparable to the power derived from the Carnot
limit. The height of the boundary layer can be expressed by the temperature difference between the surface and the top of the
935   boundary layer, using the dry adiabatic lapse rate, $\Gamma = c_p/g$, so that $z_b = c_p/g \cdot \Delta T$, with ΔT being the temperature difference
between the surface and the top of the boundary layer.

The total buoyancy production term, $G_{b,total}$ then becomes

$$G_{b,total} = \frac{1}{2} \cdot c_p \rho w' \theta' \cdot \frac{\Delta T}{\theta} \tag{C2}$$

or

940   $$G_{b,total} = \frac{1}{2} \cdot H \cdot \frac{\Delta T}{T_s} \tag{C3}$$

where H is the sensible heat flux expressed as

$$H = c_p \rho w' \theta' \tag{C4}$$

The factor of 1/2 comes from the approximately linear decrease of the buoyancy flux with height, and T_s is the approximation for the potential temperature θ of the boundary layer.

In other words, the total buoyancy production term has the form of a thermodynamic Carnot limit of a heat engine driven by the sensible heat flux, with the temperature difference between the surface and the top of the boundary layer being the driving difference. The maximization of power would have the same outcome as described in Section 2.4, except for the additional factor of 1/2, which would reduce the power, but not the outcome of the optimum heat flux or temperature difference.

Author contributions. The author wrote the whole manuscript.

Competing interests. The author declares that he has no competing interests.

Acknowledgements. The author would like to thank Anke Hildebrandt for encouragement to write this manuscript and Sarosh Alam Ghausi, Jonathan Minz, and Yinglin Tian for constructive comments.

References

Adler, R., Wang, J.-J., Sapiano, M., Huffman, G., Chiu, L., Xie, P., Ferraro, R., Schneider, U., Becker, A., Bolvin, D., Nelkin, E., and Gu, G.:
  955   NOAA CDR Program, Global Precipitation Climatology Project (GPCP) Climate Data Record (CDR), Version 2.3 (Monthly), Tech. rep.,
National Centers for Environmental Information, https://doi.org/https://doi.org/ 10.7289/V56971M6, 2016.

Arya, S. P.: Introduction to Micrometeorology, Academic Press, San Diego, CA, 1998.

Atkins, P. and de Paula, J.: Physical chemistry, Oxford Univ. Press, 9th edition edn., 2010.

Bejan, A.: Fundamentals of exergy analysis, entropy generation minimization, and the generation of flow architecture, Int. J. Energy Res.,
  960   26, 545–565, 2002.

Berner, R. A.: The rise of plants and their effect on weathering and atmospheric CO_2, Science, 276, 544–546, 1997.

Bister, M. and Emanuel, K. A.: Dissipative heating and hurricane intensity, Meteorol. Atmos. Phys., 65, 233–240, 1998.

Budyko, M. I.: The Effect of Solar Radiation Variations on the Climate of the Earth, Tellus, 21, 611–619, 1969.

Budyko, M. I.: Climate and life. Translated from the original Russian edition, Academic Press, New York., 1974.

  965   Buendia, C., Kleidon, A., Manzoni, S., Reu, B., and Porporato, A.: Evaluating the effect of nutrient redistribution by animals on the phos-
phorus cycle of lowland Amazonia, Biogeosciences, 15, 279–295, https://doi.org/10.5194/bg-15-279-2018, 2018.

Chapman, E. J., Childers, D. L., and Vallino, J. J.: How the Second Law of Thermodynamics Has Informed Ecosystem Ecology through Its
History, Bioscience, 66, 27–39, https://doi.org/10.1093/biosci/biv166, 2016.

Churkina, G. and Running, S. W.: Contrasting climatic controls on the estimated productivity of global terrestrial biomes, Ecosystems, 1,
  970   206–215, https://doi.org/10.1007/s100219900016, 1998.

Conte, L., Renner, M., Brando, P., dos Santos, C. O., Silverio, D., Kolle, O., Trumbore, S. E., and Kleidon, A.: Effects of Tropical Defor-
estation on Surface Energy Balance Partitioning in Southeastern Amazonia Estimated From Maximum Convective Power, Geophys. Res.
Lett., 46, 4396–4403, https://doi.org/10.1029/2018GL081625, 2019.

Cowan, I. R. and Farquhar, G. D.: Stomatal functioning in relation to leaf metabolism and environment, in: Integration of activity in the
  975   higher plants, edited by Jennings, D. H., pp. 471–505, Cambridge University Press, Cambridge, UK, 1977.

de Bruin, H. A. R., Trigo, I. F., Bosveld, F. C., and Meirink, J. F.: A Thermodynamically Based Model for Actual Evapotranspiration
of an Extensive Grass Field Close to FAO Reference, Suitable for Remote Sensing Application, J. Hydrometeorol., 17, 1373–1382,
https://doi.org/10.1175/JHM-D-15-0006.1, 2016.

del Jesus, M., Foti, R., Rinaldo, A., and Rodriguez-Iturbe, I.: Maximum entropy production, carbon assimilation, and the spatial organization
  980   of vegetation in river basins, Proc. Natl. Acad. Sci. USA, 109, 20 837–20 841, https://doi.org/10.1073/pnas.1218636109, 2012.

Dhara, C., Renner, M., and Kleidon, A.: Broad climatological variation of surface energy balance partitioning across land and ocean predicted
from the maximum power limit, Geophys. Res. Lett., 43, 7686–7693, https://doi.org/10.1002/2016GL070323, 2016.

Duysens, L. N. M.: The Path of Light Energy in Photosynthesis, in: Brookhaven Symposia in Biology 1: The Photochemical Apparatus, Its
Structure & Function, pp. 10–25, Brookhaven Natl. Lab., Upton, N.Y., USA, 1958.

  985   Dyke, J. G., Gans, F., and Kleidon, A.: Towards understanding how surface life can affect interior geological processes: a non-equilibrium
thermodynamics approach, Earth System Dynamics, 2, 139–160, 2011.

Emerson, R.: The quantum yield of photosynthesis, Annu. Rev. Plant. Physiol., 9, 1–24,
https://doi.org/10.1146/annurev.pp.09.060158.000245, 1958.

Enquist, B. J., Brown, J. H., and West, G. B.: Allometric scaling of plant energetics and population density, Nature, 395, 163–165, 1998.

990   Essex, C.: Minimum entropy production in the steady state and radiative transfer, Astrophys. J., 285, 279–293, 1984.

Fath, B. D., Patten, B. C., and Choi, J. S.: Complementarity of Ecological Goal Functions, J. Theor. Biol., 208, 493–506, https://doi.org/10.1006/jtbi.2000.2234, 2001.

Goody, R.: Maximum Entropy Production in climate theory, J. Atmos. Sci., 64, 2735–2739, 2007.

Hall, C. A. S.: The continuing importance of maximum power, Ecol. Mod., 178, 107–113, 2004.

995   Herrmann, W. A.: Quantifying global exergy resources, Energy, 31, 1685–1702, 2006.

Hill, R. and Rich, P. R.: A physical interpretation for the natural photosynthetic process, Proc. Natl. Acad. Sci. USA, 80, 978–982, 1983.

Holdaway, R. J., Sparrow, A. D., and Coomes, D.: Trends in entropy production during ecosystem development in the Amazon basin, Phil. Trans. R. Soc. B, 365, 1437–1447, 2010.

Holdridge, L. R.: Determination of world plant formations from simple climatic data, Science, 105, 367–368, 1947.

1000   Joergensen, S. E.: Toward a Consistent Pattern of Ecosystem Theories, The Scientific World, 1, 71–75, https://doi.org/10.1100/tsw.2001.15, 2001.

Jupp, T. E. and Cox, P. M.: MEP and planetary climates: insights from a two-box climate model containing atmospheric dynamics, Phil. Trans. R. Soc. B, 365, 1355–1365, 2010.

Kabelac, S.: Thermodynamik der Strahlung, Vieweg, Braunschweig and Wiesbaden, 1994.

1005   Kasting, J. F. and Catling, D.: Evolution of a habitable planet, Annu. Rev. Astron. Astrophys., 41, 429–463, 2003.

Kato, S., Rose, F. G., Rutan, D. A., Thorsen, T. J., Loeb, N. G., Doelling, D. R., Huang, X., Smith, W. L., Su, W., and Ham, S.-H.: Surface Irradiances of Edition 4.0 Clouds and the Earth's Radiant Energy System (CERES) Energy Balanced and Filled (EBAF) Data Product, J. Clim., 31, 4501–4527, https://doi.org/10.1175/JCLI-D-17-0523.1, 2018.

Katul, G. G., Palmroth, S., and Oren, R.: Leaf stomatal responses to vapour pressure deficit under current and CO2-enriched atmosphere
1010   explained by the economics of gas exchange, Plant Cell Env., 32, 968–979, https://doi.org/10.1111/j.1365-3040.2009.01977.x, 2009.

Kleidon, A.: Life, Hierarchy, and the Thermodynamic Machinery of Planet Earth, Physics of Life Reviews, 7, 424–460, 2010.

Kleidon, A.: How does the Earth system generate and maintain thermodynamic disequilibrium and what does it imply for the future of the planet?, Phil. Trans. R. Soc. A, 370, 1012–1040, 2012.

Kleidon, A.: Thermodynamic foundations of the Earth system, Cambridge University Press, 2016.

1015   Kleidon, A.: Physical limits of wind energy within the atmosphere and its use as renewable energy: From the theoretical basis to practical implications, Meteorol. Z., 30, 203–225, https://doi.org/10.1127/metz/2021/1062, 2021a.

Kleidon, A.: What limits photosynthesis? Identifying the thermodynamic constraints of the terrestrial biosphere within the Earth system, BBA Bioenergetics, 1862, 148 303, https://doi.org/10.1016/j.bbabio.2020.148303, 2021b.

Kleidon, A.: Understanding the Earth as a Whole System: From the Gaia Hypothesis to Thermodynamic Optimality and Human Societies,
1020   in: Kosmos. Vom Umgang mit der Welt zwischen Ausdruck und Ordnung, edited by König, P. and Schlaudt, O., Heidelberg Univ. Press, in press.

Kleidon, A. and Heimann, M.: A method of determining rooting depth from a terrestrial biosphere model and its impacts on the global water- and carbon cycle, Global Change Biol., 4, 275–286, 1998.

Kleidon, A. and Renner, M.: Thermodynamic limits of hydrologic cycling within the Earth system: concepts, estimates and implications,
1025   Hydrol. Earth Syst. Sci., 17, 2873–2892, 2013a.

Kleidon, A. and Renner, M.: A simple explanation for the sensitivity of the hydrologic cycle to climate change, Earth Syst. Dynam., 4, 455–465, https://doi.org/10.5194/esd-4-455-2013, 2013b.

Kleidon, A. and Renner, M.: An explanation for the different climate sensitivities of land and ocean surfaces based on the diurnal cycle, Earth Syst. Dynam., 8, 849–864, https://doi.org/10.5194/esd-8-849-2017, 2017.

Kleidon, A. and Renner, M.: Diurnal land surface energy balance partitioning estimated from the thermodynamic limit of a cold heat engine, Earth Syst. Dynam., 9, 1127–1140, https://doi.org/10.5194/esd-9-1127-2018, 2018.

Kleidon, A. and Schymanski, S.: Thermodynamics and optimality of the water budget on land: A review, Geophys. Res. Lett., 35, L20 404, 2008.

Kleidon, A., Zehe, E., Ehret, U., and Scherer, U.: Thermodynamics, maximum power, and the dynamics of preferential river flow structures on continents, Hydrol. Earth Syst. Sci., 17, 225–251, 2013.

Kleidon, A., Kravitz, B., and Renner, M.: The hydrological sensitivity to global warming and solar geoengineering derived from thermodynamic constraints, Geophys. Res. Lett., 42, https://doi.org/10.1002/2014GL062589, 2015a.

Kleidon, A., Miller, L., and Gans, F.: Physical limits of solar energy conversion in the Earth system, Top. Curr. Chem., in press, 2015b.

Koeppen, W.: Versuch einer Klassifikation der Klimate, vorzugsweise nach ihren Beziehungen zur Pflanzenwelt, Geogr. Z., 6, 593–611, https://www.jstor.org/stable/27803924, 1900.

Koll, D. D. B. and Cronin, T. W.: Earth's outgoing longwave radiation linear due to H2O greenhouse effect, Proc. Natl. Acad. Sci. USA, 115, 10 293–10 298, 2018.

Kondepudi, D. and Prigogine, I.: Modern thermodynamics - from heat engines to dissipative structures, Wiley, Chichester, 1998.

Landsberg, P. T. and Tonge, G.: Thermodynamics of the conversion of diluted radiation, J. Phys. A, 12, 551–562, 1979.

Landsberg, P. T. and Tonge, G.: Thermodynamic energy conversion efficiencies, Journal of Applied Physics, 51, R1, 1980.

Law, B. E., Falge, E., Gu, L., Baldocchi, D. D., Bakwin, P., Berbigier, P., Davis, K., Dolman, A. J., Falk, M., Fuentes, J. D., Goldstein, A., Granier, A., Grelle, A., Hollinger, D., Janssens, I. A., Jarvis, P., Jensen, N. O., Katul, G., Malhi, Y., Matteucci, G., Meyers, T., Monson, R., Munger, W., Oechel, W., Olson, R., Pilegaard, K., U, K. T. P., Thorgeirsson, H., Valentini, R., Verman, S., Vesala, T., Wilson, K., and Wofsy, S.: Environmental controls over carbon dioxide and water vapor exchange of terrestrial vegetation, Agric. For. Meteor., 113, 97–120, 2002.

Li, L., Ingersoll, A. P., Jiang, X., Feldman, D., and Yung, Y. L.: Lorenz energy cycle of the global atmosphere based on reanalysis datasets, Geophys. Res. Lett., 34, L16 813, 2007.

Lin, H.: Linking principles of soil formation and flow regimes, J. Hydrol., in press, 2010.

Lineweaver, C. H. and Egan, C. A.: Life, gravity and the second law of thermodynamics, Physics of Life Reviews, 5, 225–242, 2008.

Loeb, N. G., Doelling, D. R., Wang, H., Su, W., Nguyen, C., Corbett, J. G., Liang, L., Mitrescu, C., Rose, F. G., and Kato, S.: Clouds and the Earth's Radiant Energy System (CERES) Energy Balanced and Filled (EBAF) Top-of- Atmosphere (TOA) Edition 4.0 Data Product, J. Clim., 31, 895–918, https://doi.org/10.1175/JCLI-D-17-0208.1, 2018.

Lorenz, E. N.: Available potential energy and the maintenance of the general circulation, Tellus, 7, 157–167, 1955.

Lorenz, E. N.: Generation of available potential energy and the intensity of the general circulation, in: Dynamics of Climate, edited by Pfeffer, R. C., pp. 86–92, Pergamon Press, Oxford, UK, 1960.

Lorenz, E. N.: The Nature and Theory of the General Cir- culation of the Atmosphere, WMO, Geneva, 1967.

Lorenz, R. D., Lunine, J. I., Withers, P. G., and McKay, C. P.: Titan, Mars and Earth: Entropy production by latitudinal heat transport, Geophys. Res. Lett., 28, 415–418, 2001.

Lotka, A. J.: Contribution to the Energetics of Evolution, Proc. Natl. Acad. Sci. U.S.A., 8, 147–151, 1922a.

Lotka, A. J.: Natural Selection as a Physical Principle, Proc. Natl. Acad. Sci. U.S.A., 8, 151–154, 1922b.

Lotka, A. J.: Elements of physical biology, Williams and Wilkins, Baltimore, USA, 1925.

Lovelock, J. E.: A Physical Basis for Life Detection Experiments, Nature, 207, 568–570, 1965.

Lovelock, J. E.: Gaia as Seen Through the Atmosphere, Atmos. Environ., 6, 579–580, 1972a.

Lovelock, J. E.: Gaia: A New Look at Life on Earth, Oxford University Press, Oxford, UK, 1972b.

1070 Margules, M.: Über die Energie der Stürme, Jahrb. Zentralanst. Meteorol., 40, 1–26, 1905.

Martens, B., Miralles, D., Lievens, H., van der Schalie, R., de Jeu, R., Fernández-Prieto, D., Beck, H., Dorigo, W., and Verhoest, N.: GLEAM v3: satellite-based land evaporation and root-zone soil moisture, Geosci. Model Dev., 10, 1903–1925, https://doi.org/10.5194/gmd-10-1903-2017, 2017.

McNaughton, S. J.: Grazing as an optimization process: grass-ungulate relationships in the Serengeti, Am. Nat., 113, 691–703, 1979.

1075 Medlyn, B. E., Duursma, R. A., Eamus, D., Ellsworth, D. S., Prentice, I. C., Barton, C. V. M., Crous, K. Y., de Angelis, P., Freemand, M., and Wingate, L.: Reconciling the optimal and empirical approaches to modelling stomatal conductance, Global Change Biol., 17, 2134–2144, https://doi.org/10.1111/j.1365-2486.2010.02375.x, 2011.

Miguez-Macho, G. and Fan, Y.: The role of groundwater in the Amazon water cycle: 2. Influence on seasonal soil moisture and evapotranspiration, J. Geophys. Res., 117, D15 114, https://doi.org/10.1029/2012JD017540, 2012.

1080 Miller, L. M. and Kleidon, A.: Wind speed reductions by large-scale wind turbine deployments lower turbine efficiencies and set low generation limits, Proc. Natl. Acad. Sci. USA, 113, 13 570–13 575, https://doi.org/10.1073/pnas.1602253113, 2016.

Miller, L. M., Gans, F., and Kleidon, A.: Estimating maximum global land surfacw wind power extractability and associated climatic consequences, Earth System Dynamics, 2, 1–12, 2011.

Miralles, D., Holmes, T., de Jeu, R., Gash, J., Meesters, A., and Dolman, A.: Global land-surface evaporation estimated from satellite-based 1085 observations, Hydrol. Earth Syst. Sci., 15, 453–469, https://doi.org/10.5194/ hess-15-453-2011, 2011.

Monteith, J. L.: Light distribution and photosynthesis in field crops, Ann. Bot., 29, 17–37, 1965.

Monteith, J. L.: Solar radiation and productivity in tropical ecosystems, J. Appl. Ecol., 9, 747–766, 1972.

Monteith, J. L.: Climate and the efficiency of crop production in Britain, Phil. Trans. R. Soc. B, 281, 277–294, 1977.

Nepstad, D. C., de Carvalho, C. R., Davidson, E. A., Jipp, P. H., Lefebvre, P. A., Negreiros, H. G., da Silva, E. D., Stone, T. A., Trumbore, 1090 S. E., and Vieira, S.: The role of deep roots in the hydrological and carbon cycles of Amazon forests and pastures, Nature, 372, 666–669, 1994.

Nielsen, S. N., Müller, F., Marques, J. C., Bastianoni, S., and Joergensen, S. E.: Thermodynamics in Ecology—An Introductory Review, Entropy, 22, 820, https://doi.org/10.3390/e22080820, 2020.

Odum, H. T.: Self-organization, transformity, and information, Science, 242, 1132–1139, 1988.

1095 Odum, H. T. and Pinkerton, R. C.: Time's speed regulator: the optimum efficiency for maximum power output in physical and biological systems, Amer. Scientist, 43, 331–343, 1955.

Ott, L.: GEOS-Carb CASA-GFED 3-Hourly Ecosystem Exchange Fluxes 0.5 Degree x 0.625 Degree, Tech. rep., Goddard Earth Sciences Data and Information Services Center (GES DISC), Greenbelt, MD, USA, https://doi.org/10.5067/VQPRALE26L20, 2020.

Ozawa, H., Ohmura, A., Lorenz, R. D., and Pujol, T.: The second law of thermodynamics and the global climate system – A review of the 1100 Maximum Entropy Production principle, Rev. Geophys., 41, 1018, 2003.

Paltridge, G. W.: Global dynamics and climate – a system of minimum entropy exchange, Q. J. Roy. Meteorol. Soc., 101, 475–484, 1975.

Paltridge, G. W.: The steady-state format of global climate, Q. J. Roy. Meteorol. Soc., 104, 927–945, 1978.

Paltridge, G. W.: Climate and thermodynamic systems of maximum dissipation, Nature, 279, 630–631, 1979.

Peixoto, J. P. and Oort, A. H.: Physics of Climate, American Institute of Physics, New York, NY, 1992.

1105 Penman, H. L.: Natural evaporation from open water, bare soil, and grass, Proc. R. Soc. London A, 193, 120–146, 1948.

Petela, R.: Exergy of heat radiation, J. Heat Transfer, 86, 187–192, 1964.

Porada, P., Kleidon, A., and Schymanski, S. J.: Entropy production of soil hydrological processes and its maximization, Earth Syst. Dynam., 2, 179–190, 2011.

Prentice, I. C., Cramer, W., Harrison, S. P., Leemans, R., Monserud, R. A., and Solomon, A. M.: A global biome model based on plant
1110   physiology and dominance, soil properties and climate, J. Biogeography, 19, 117–134, 1992.

Press, W. H.: Theoretical maximum for energy from direct and diffuse sunlight, Nature, 264, 734–735, 1976.

Priestley, C. H. B. and Taylor, R. J.: On the assessment of surface heat flux and evaporation using large-scale parameters, Mon. Wea. Rev., 100, 81–92, 1972.

Prigogine, I.: Introduction to Thermodynamics of Irreversible Processes, Thournes, Chicago, 1955.

1115 Radmer, R. and Kok, B.: Photosynthesis: limited yields, unlimited dreams, Bioscience, 27, 599–605, 1977.

Randerson, J., van der Werf, G., Giglio, L., Collatz, G., and Kasibhatla, P.: Global Fire Emissions Database, Version 4.1 (GFEDv4), Tech. rep., ORNL DAAC, Oak Ridge, Tennessee, USA, https://doi.org/10.3334/ORNLDAAC/1293, 2017.

Renno, N. O. and Ingersoll, A. P.: Natural convection as a heat engine: A theory for CAPE, J. Atmos. Sci., 53, 572–585, 1996.

Rinaldo, A., Rodriguez-Iturbe, I., Rigon, R., Bras, R. L., Ijjasz-Vasquez, E., and Marani, A.: Minimum energy and fractal structures of
1120   drainage networks, Water Resour. Res., 28, 2183–2195, 1992.

Rinaldo, A., Maritan, A., Colaiori, F., Flammini, A., Rigon, R., Rodriguez-Iturbe, I., and Banavar, J. R.: Thermodynamics of fractal networks, Phys. Rev. Lett., 76, 3364–3367, 1996.

Rodriguez-Iturbe, I. and Rinaldo, A.: Fractal River Basins: Chance and Self-Organization, Cambridge University Press, Cambridge, UK, 1997.

1125 Rosen, M. A. and Scott, D. S.: Entropy production and exergy destruction: Part I - hierarchy of Earth's major constituencies, Int. J. Hydrogen Energ., 28, 1307–1313, 2003.

Rubin, D. M. and Hunter, R. E.: Bedform alignment in directionally varying flows, Science, 237, 276–278, 1987.

Savenije, H. H. G. and Hrachowitz, M.: HESS Opinions "Catchments as meta-organisms – a new blueprint for hydrological modelling", Hydrology and Earth System Sciences, 21, 1107–1116, https://doi.org/10.5194/hess-21-1107-2017, 2017.

1130 Schimel, D., Stephens, B. B., and Fisher, J. B.: Effect of increasing CO2 on the terrestrial carbon cycle, Proc. Natl. Acad. Sci. USA, 112, 436–441, https://doi.org/10.1073/pnas.1407302112, 2015.

Schmidt, W.: Strahlung und Verdunstung an freien Wasserflächen; ein Beitrag zum Wärmehaushalt des Weltmeeres und zum Wasserhaushalt der Erde, Ann. d. Hydrogr. u. maritimen Meteorol., 43, 111–178, 1915.

Schneider, E. D. and Kay, J. J.: Life as a manifestation of the second law of thermodynamics, Math. Comput. Modeling, 19, 25–48, 1994.

1135 Schrödinger, E.: What is Life? The physical aspect of the living cell, Cambridge University Press, Cambridge, UK, 1944.

Schwartzman, D. W. and Volk, T.: Biotic enhancement of weathering and the habitability of Earth, Nature, 340, 457–460, 1989.

Schymanski, S. J., Kleidon, A., Stieglitz, M., and Narula, J.: Maximum entropy production allows a simple representation of heterogeneity in semiarid ecosystems, Phil. Trans. R. Soc. B, 365, 2010.

Singh, M. S. and O'Neill, M. E.: The climate system and the second law of thermodynamics, Rev. Mod. Phys., 94,
1140   https://doi.org/10.1103/RevModPhys.94.015001, 2022.

Slayter, R. O. and McIlroy, I. C.: Practical Micrometeorology, 310 pp., CSIRO, Melbourne, Australia, 1961.

Stull, R. B.: An introduction to boundary layer meteorology, Kluwer Academic Press, Boston, USA, 1989.

Tailleux, R.: Available Potential Energy and exergy in stratified fluids, Annu. Rev. Fluid Mech., 45, 35–58, 2013.

Tu, Z., Yang, Y., and Roderick, M. L.: Testing a maximum evaporation theory over saturated land: implications for potential evaporation estimation, Hydrol. Earth Syst. Sci., 26, 1745–1754, https://doi.org/10.5194/hess-26-1745-2022, 2022.

Ulanowicz, R. E. and Hannon, B. M.: Life and the production of entropy, Proc. R. Soc. Lond. B, 232, 181–192, 1987.

Vanni, M. J.: Nutrient cycling by animals in freshwater ecosystems, Annu. Rev. Ecol. Syst., 33, 341–370, 2002.

von Humboldt, A.: Kosmos. Entwurf einer physischen Weltanschauung, J. G Cotta, Stuttgart, 1845.

Wang, J. and Bras, R. L.: A model of evapotranspiration based on the theory of maximum entropy production, Water Resour. Res., 47, W03 521, 2011.

Wang, J., Salvucci, G. D., and Bras, R. L.: An extremum principle of evaporation, Water Resour. Res., 40, 2004.

Wang, J., Bras, R. L., Lerdau, M., and Salvucci, G. D.: A maximum hypothesis of transpiration, J. Geophys. Res., 112, 2007.

Wang-Erlandsson, L., Bastiaanssen, W. G. M., Gao, H., Jägermeyr, J., Senay, G. B., van Dijk, A. I. J. M., Guerschman, J. P., Keys, P. W., Gordon, L. J., and Savenije, H. H. G.: Global root zone storage capacity from satellite-based evaporation, Hydrology and Earth System Sciences, 20, 1459–1481, https://doi.org/10.5194/hess-20-1459-2016, 2016.

West, G. B., Brown, J. H., and Enquist, B. J.: A general model for the origin of allometric scaling laws in biology, Science, 276, 122–126, 1997.

West, G. B., Brown, J. H., and Enquist, B. J.: A general model for the structure and allometry of plant vascular systems, Nature, 400, 664–667, 1999.

Whittaker, R. H.: Classification of natural communities, Bot. Rev., 28, 1–239, 1962.

Wolf, A., Doughty, C. E., and Malhi, Y.: Lateral Diffusion of Nutrients by Mammalian Herbivores in Terrestrial Ecosystems, PLOS ONE, 8, e71 352, https://doi.org/10.1371/journal.pone.0071352, 2013.

Wu, W. and Liu, Y.: Radiation entropy flux and entropy production of the Earth system, Rev. Geophys., 48, RG2003, 2010.

Yang, Y. and Roderick, M. L.: Radiation, surface temperature and evaporation over wet surfaces, Q. J. R. Meteorol. Soc., 145, 1118–1129, https://doi.org/10.1002/qj.3481, 2019.

Zehe, E., Ehret, U., Blume, T., Kleidon, A., Scherer, U., and Westhoff, M.: A thermodynamic approach to link self-organization, preferential flow and rainfall–runoff behaviour, Hydrol. Earth Syst. Sci., 17, 4297–4322, https://doi.org/10.5194/hess-17-4297-2013, 2013.